

1 **Estradiol-inducible AvrRps4 expression reveals distinct properties of**
2 **TIR-NLR-mediated effector-triggered immunity**

3

4 Bruno Pok Man Ngou^{1,2}, Hee-Kyung Ahn^{1,2}, Pingtao Ding^{1,2,*}, Amey Redkar^{1,3},
5 Hannah Brown¹, Yan Ma¹, Mark Youles¹, Laurence Tomlinson¹, Jonathan DG
6 Jones^{1,*}

7

8 1 The Sainsbury Laboratory, Norwich Research Park, Norwich NR4 7UH, UK

9 2 These authors contributed equally to this work

10 3 Department of Genetics, University of Córdoba, Córdoba 14071, Spain

11

12 * For correspondence: pingtao.ding@tsl.ac.uk; jonathan.jones@tsl.ac.uk

13

14 **Highlight**

15 Inducible expression of AvrRps4 activates RRS1/RPS4-mediated effector-
16 triggered immunity without the presence of pathogens, allowing us to
17 characterise downstream immune responses triggered by TIR-NLRs without
18 cell-surface receptor-mediated immunity.

19

20 **Abstract**

21 Plant nucleotide-binding domain, leucine-rich repeat receptor (NLR) proteins
22 play important roles in recognition of pathogen-derived effectors. However, the
23 mechanism by which plant NLRs activate immunity is still largely unknown. The
24 paired Arabidopsis NLRs RRS1-R and RPS4, that confer recognition of
25 bacterial effectors AvrRps4 and PopP2, are well studied, but how the
26 RRS1/RPS4 complex activates early immediate downstream responses upon
27 effector detection is still poorly understood. To study RRS1/RPS4 responses
28 without the influence of cell-surface receptor immune pathways, we generated
29 an Arabidopsis line with inducible expression of effector AvrRps4. Induction
30 does not lead to hypersensitive cell death response (HR) but can induce
31 electrolyte leakage, which often correlates with plant cell death. Activation of
32 RRS1 and RPS4 without pathogens cannot activate mitogen-associated

33 protein kinase cascades, but still activates upregulation of defence genes, and
34 therefore resistance against bacteria.

35

36 **Keywords**

37 Plant innate immunity, NLR activation, protein complex, hypersensitive
38 response, cell death, MAP kinase, defence gene expression, estradiol-
39 inducible expression system, Golden Gate modular cloning

40

41 **Introduction**

42 To investigate plant immunity, researchers routinely conduct pathogen
43 inoculations on plants in a controlled environment. Upon pathogen attack,
44 plants activate innate immune responses via both membrane-associated and
45 intracellular receptors, which makes it difficult to unravel the distinct contribution
46 of each component. Most plasma-membrane localized receptors perceive
47 conserved pathogen-associated molecular patterns (PAMPs) or host-cell-
48 derived damage-associated molecular patterns (DAMPs) and activate PAMP-
49 triggered immunity (PTI) or DAMP-triggered immunity (DTI). Plant intracellular
50 immune receptors belong to a family of nucleotide-binding leucine-rich repeat
51 (NB-LRR) proteins, also known as NLRs. NLRs recognize pathogen effectors
52 and activate effector-triggered immunity (ETI), which often leads to
53 accumulation of reactive oxygen species (ROS) and a hypersensitive cell death
54 response (HR). Most plant NLRs carry either coiled-coil (CC) or Toll/interleukin-
55 1 receptor (TIR) N-terminal domains. Both CC and TIR domains are believed
56 to function in signalling upon activation of NLRs, but the detailed mechanisms
57 are unknown. Many CC-NLRs localize at and function in association with the
58 plasma membrane, whereas TIR-NLRs can function in diverse locations,
59 including the nucleus. Regardless of the distinct localization patterns between
60 CC- and TIR-NLRs, their downstream outputs culminate in elevated resistance,
61 but have never been directly compared side-by-side. To study the specific
62 immune outputs generated by ETI, inducible expression tools have been
63 applied (McNellis *et al.*, 1998; Tornero *et al.*, 2002; Allen *et al.*, 2004; Porter *et*
64 *al.*, 2012).

65 In Arabidopsis, functionally paired NLRs RRS1-R and RPS4 confer resistance
66 against a soil-borne bacterial pathogen *Ralstonia solanacearum* through the

67 recognition of an effector PopP2 secreted via Type III secretion system and a
68 hemibiotrophic ascomycetous fungal pathogen *Colletotrichum higginsianum*
69 (Narusaka *et al.*, 2009). They can also confer resistance against bacteria
70 *Pseudomonas syringae* pv. *tomato* DC3000 carrying AvrRps4, an effector
71 protein from *Pseudomonas syringae* pv. *pisi*, causing bacterial blight in *Pisum*
72 *sativum* (pea) (Sohn *et al.*, 2009; Narusaka *et al.*, 2009). Previously, it was
73 reported that the 135th to 138th residues of AvrRps4, lysine-arginine-valine-
74 tyrosine (KRVY), are required for the recognition of AvrRps4 by RRS1 and
75 RPS4 (Sohn *et al.*, 2009). Crystal structure of the C-terminus of AvrRps4
76 revealed that the 187th residue glutamate (E187) is also required for HR and
77 immunity (Sohn *et al.*, 2012). PopP2 recognition by RRS1 occurs by the
78 integrated WRKY domain at the C-terminal of a resistant allele of RRS1-R (from
79 the Ws-2 ecotype of Arabidopsis) but not the susceptible allele of RRS1-S (from
80 the Col-0 ecotype of Arabidopsis) (Sarris *et al.*, 2015). Crystal structure
81 information of RRS1 and RPS4 on the TIR domains and the co-crystal
82 structures between RRS1-R WRKY domain and effector PopP2 have indicated
83 some structural basis of how RRS1/RPS4 have been activated (Williams *et al.*,
84 2014; Zhang *et al.*, 2017). However, it is still unknown how the protein complex
85 assembles and functions.

86 Here we report tools for studying the immune complex of RRS1-R and RPS4 *in*
87 *vivo*. We established a set of transgenic Arabidopsis lines to study
88 RRS1/RPS4-mediated ETI in the absence of pathogens. Using these lines, we
89 show that some but not all immune outputs induced by the conditionally
90 expressed AvrRps4 resemble other reported effector-inducible lines.

91

92 **Materials and Methods**

93 *Plant material and growth conditions*

94 *Arabidopsis thaliana* accessions Wassilewskija-2 (Ws-2) and Columbia-0 (Col-
95 0) were used as wild type in this study. The *eds1-2* mutant used has been
96 described previously (Falk *et al.*, 1999). Seeds were sown on compost and
97 plants were grown at 21°C with 10 hours under light and 14 hours in dark (10h-
98 L/14h-D), and at 70% humidity. Tabaco plants were grown at 22°C with 16h-
99 L/8h-D, and at 80% constant humidity. The light level is approximately 180-200
100 μmol s with fluorescent tubes.

101

102 *FastRed selection for transgenic Arabidopsis*

103 Seeds harvested from the Agrobacteria-transformed Arabidopsis are
104 resuspended in 0.1% Agarose and exposed under fluorescence microscope
105 with DsRed (red fluorescent protein) filter. Seeds with bright red fluorescence
106 are selected as the positive transformants.

107

108 *GUS staining*

109 *Nicotiana benthamiana* (*N. b.*) leaves were infiltrated with Agrobacteria carrying
110 constructs with β -glucuronidase (GUS) reporter gene expressed under selected
111 Arabidopsis promoters (Table S1). Leaves were collected at 2 days post
112 infiltration (dpi), and vacuum-infiltrated with GUS staining buffer (0.1 M sodium
113 phosphate pH 7.0, 10 mM EDTA pH 7.0, 0.5 mM $K_3Fe(CN)_6$, 0.5 mM $K_4Fe(CN)_6$,
114 0.76 mM 5-Bromo-4-chloro-3-indolyl- β -D-glucuronide cyclohexylamine salt or
115 X-Gluc, and 0.04% Triton X-100). After vacuum-infiltration, the leaves were
116 incubated at 37°C overnight in the dark. The leaves were rinsed with 70%
117 ethanol until the whole leaf de-stains to a clear white.

118

119 *Immunoblotting*

120 *N. b.* leaves were infiltrated with Agrobacteria carrying our stacking constructs
121 (Table S2). At 2 dpi, same leaves were infiltrated with either DMSO or 50 μ M
122 β -estradiol (E2) diluted in water. Samples were collected at 6 hpi of DMSO or
123 E2 treatment, and snap-frozen in liquid nitrogen. Proteins were extracted using
124 GTEN buffer (10% glycerol, 25 mM Tris pH 7.5, 1 mM EDTA, 150 mM NaCl)
125 with 10 mM DTT, 1% NP-40 and protease inhibitor cocktail (cOmplete™,
126 EDTA-free; Merck). For *Arabidopsis* seedlings, seedlings grown for 8 days after
127 germination were treated with DMSO or E2 with indicated time points and snap-
128 frozen in liquid nitrogen. After centrifugation at 13,000 rpm for 15 minutes to
129 remove cell debris, protein concentration of each sample was measured using
130 the Bradford assay (Protein Assay Dye Reagent Concentrate; Bio-Rad). After
131 normalization, extracts were incubated with 3 \times SDS sample buffer at 95°C for
132 5 minutes. 6% SDS-PAGE gels were used to run the protein samples. After
133 transferring proteins from gels to PVDF membranes (Merck-Millipore) using
134 Trans-Blot Turbo System (Bio-Rad), membranes were immunoblotted with

135 HRP-conjugated Flag antibodies (Monoclonal ANTI-FLAG® M2-Peroxidase
136 HRP antibody produced in mouse, A5892; Merck-Millipore), HRP-conjugated
137 HA antibodies (12013819001; Merck-Roche) or Phospho-p44/42 MAPK
138 (Erk1/2) (Thr202/Tyr204) (D13.14.4E) XP® Rabbit monoclonal antibody (4370;
139 Cell Signalling Technology). Anti-Rabbit IgG (whole molecule)–Peroxidase
140 antibody produced in goat (A0545; Merck-Sigma-Aldrich) was used as
141 secondary antibody following the use of Phospho-p44/42 MAPK antibody.

142

143 *Bacterial growth assay*

144 *Pseudomonas syringae* pv. *tomato* strain DC3000 carrying pVSP61 empty
145 vector was grown on selective King's B (KB) medium plates containing 15%
146 (w/v) Agar, 25 µg/ml rifampicin and 50 µg/ml kanamycin for 48 h at 28°C.
147 Bacteria were harvested from the plates, resuspended in infiltration buffer (10
148 mM MgCl₂) and the concentration was adjusted to an optical density of 0.001
149 at 600 nm (OD₆₀₀=0.001, representing approximately 5×10⁵ colony forming
150 units [CFU] ml⁻¹). Bacteria were infiltrated into abaxial surfaces of 5-week-old
151 Arabidopsis leaves with a 1-ml needleless syringe. For quantification, leaf
152 samples were harvested with a 6-mm-diameter cork borer (Z165220; Merck-
153 Sigma-Aldrich), resulting in leaf discs with an area of 0.283 cm². Two leaf discs
154 per leaf were harvested as a single sample. For each condition, four samples
155 were collected immediately after infiltration as 'day 0' samples to ensure no
156 significant difference introduced by unequal infiltrations and six samples were
157 collected at 3 dpi as 'day 3' samples to compare the bacteria growth between
158 different genotypes, conditions and treatments. For 'day 0', samples were
159 ground in 200 µl of infiltration buffer and spotted (10 µl per spot) on selective
160 KB medium agar plates to grow for 48 h at 28°C. For 'day 3', samples were
161 ground in 200 µl of infiltration buffer, serially diluted (5, 50, 500, 5000 and 50000
162 times) and spotted (6 µl per spot) on selective KB medium agar plates to grow
163 for 48 h at 28°C. The number of colonies (CFU per drop) was monitored and
164 bacterial growth was represented as in CFU cm⁻² of leaf tissue. All results are
165 plotted using ggplot2 in R (Wickham, 2016), and detailed statistics summary
166 can be found in the supplemental materials.

167

168 *HR phenotyping in Arabidopsis*

169 *Pseudomonas fluorescens* engineered with a type III secretion system (Pf0-1
170 'EtHAn' strains) expressing one of wild-type or mutant effectors, AvrRps4,
171 AvrRps4^{KRVY135-138AAAA}, PopP2, PopP2^{C321A}, AvrRpt2 or pVSP61 empty vector
172 were grown on selective KB plates for 24 h at 28°C (Thomas *et al.*, 2009; Sohn
173 *et al.*, 2014). Bacteria were harvested from the plates, resuspended in
174 infiltration buffer (10 mM MgCl₂) and the concentration was adjusted to OD₆₀₀=
175 0.2 (10⁸ CFU ml⁻¹). The abaxial surfaces of 5-week-old Arabidopsis leaves were
176 hand infiltrated with a 1-ml needleless syringe. Cell death was monitored 24 h
177 after infiltration.

178

179 *Electrolyte leakage assay*

180 Either 50 µM E2 or DMSO were hand infiltrated in 5-week-old Arabidopsis
181 leaves with a 1-ml needleless syringe for electrolyte leakage assay. Leaf discs
182 were taken with a 2.4-mm-diameter cork borer from infiltrated leaves. Discs
183 were dried and washed in deionized water for 1 hour before being floated on
184 deionized water (15 discs per sample, three samples per biological replicate).
185 Electrolyte leakage was measured as water conductivity with a Pocket Water
186 Quality Meters (LAQUAtwin-EC-33; Horiba) at the indicated time points. All
187 results are plotted using ggplot2 in R (Wickham, 2016) , and detailed statistics
188 summary can be found in the supplemental materials.

189

190 *Trypan blue staining*

191 Either 50 µM E2 or DMSO were hand infiltrated in 5-week-old Arabidopsis
192 leaves with a 1-ml needleless syringe for trypan blue staining. 6 leaves per
193 sample were collected 24 hours after infiltration. Leaves were boiled in trypan
194 blue solution (1.25 mg/ml trypan blue dissolved in 12.5% glycerol, 12.5%
195 phenol, 12.5% lactic acid and 50% ethanol) in a boiling water bath for 1 min
196 and de-stained by chloral hydrate solution (2.5 g/ml). De-stained leaves were
197 mounted, and pictures were taken under on Leica fluorescent
198 stereomicroscope M165FC. All images were taken with identical settings at
199 2.5x magnification. Scale bar=0.5mm.

200

201 *Reverse transcription-quantitative polymerase chain reaction (RT-qPCR) for*
202 *measuring relative gene expression*

203 For gene expression analysis, RNA was isolated from 5-week-old Arabidopsis
204 leaves and used for subsequent RT-qPCR analysis. RNA was extracted with
205 Quick-RNA Plant Kit (R2024; Zymo Research) and treated with RNase-free
206 DNase (4716728001; Merck-Roche). Reverse transcription was carried out
207 using SuperScript IV Reverse Transcriptase (18090050; ThermoFisher
208 Scientific). qPCR was performed using a CFX96 Touch™ Real-Time PCR
209 Detection System. Primers for qPCR analysis of *Isochorismate Synthase1*
210 (*ICS1*), *Pathogenesis-Related1 (PR1)*, *AvrRps4* and *Elongation Factor 1 Alpha*
211 (*EF1 α*) are listed in Table S4. Data were analyzed using the double delta Ct
212 method (Livak and Schmittgen, 2001). All results are plotted using ggplot2 in R
213 (Wickham, 2016), and detailed statistics summary can be found in the
214 supplemental materials.

215

216 *Confocal laser scanning microscopy (CLSM) imaging*

217 Transgenic plant materials were imaged with the Leica DM6000/TCS SP5
218 confocal microscopy (Leica Microsystems) for confirmation of expression of
219 inducible AvrRps4 fused with monomeric yellow-green fluorescent protein,
220 mNeonGreen or mNeon (Shaner *et al.*, 2013). Roots from 3-week-old
221 Arabidopsis seedlings were sprayed with 50 μ M E2 and imaged at 1 day post
222 spray. Fluorescence of mNeon was excited at 500 nm and detected at between
223 520 and 540 nm. CLSM images of root cells from Arabidopsis seedlings are
224 recorded via the camera. The images were analyzed with the Leica application
225 Suite and Fiji software (Schindelin *et al.*, 2012).

226

227 *Co-immunoprecipitation*

228 Arabidopsis transgenic seedlings, and the background ecotype Col-0 grown for
229 7 days after germination (DAG) were treated with 0.1% DMSO or 50 μ M E2 for
230 3 hours. Proteins from seedlings were extracted using IP buffer (10% Glycerol,
231 50mM Tris-Cl pH 6.8, 50mM KCl, 1mM EDTA, 5mM MgCl₂, 1% NP-40, 10mM
232 DTT, 1mM dATP). Crude extract of the seedlings was centrifuged, and
233 supernatants were incubated with Anti-HA-conjugated beads (EZview™ Red
234 Anti-HA Affinity Gel; E6779; Sigma). A small portion of supernatants were taken
235 for input samples. At 2 hours after incubation of the extract with beads, beads
236 were washed three times with IP buffer containing 0.1% NP-40. Proteins bound

237 to beads were eluted by boiling the beads with SDS sample buffer.
238 Immunoblotting of the input and eluted samples were performed as described
239 above.

240

241 **Results**

242 **RRS1 over-expression can compromise RPS1/RPS4 function**

243 Overexpression of *RPS4* leads to autoimmunity and dwarfism under standard
244 growth condition (see Materials and Methods) (Heidrich *et al.*, 2013). This
245 autoimmunity is both temperature- and RRS1-dependent. In contrast, elevated
246 expression of *RRS1-R* from ecotype Ws-2 in Col-0, an ecotype expressing a
247 dominant allele of *RRS1-S*, does not trigger auto-immunity (Huh *et al.*, 2017).
248 Furthermore, high level RRS1-R expression does not confer recognition of
249 effector PopP2 (Fig 1). Overexpression of *RRS1* in an *RPS4* overexpression
250 line attenuates dwarfism and autoimmunity (Huh *et al.*, 2017). We infiltrated
251 non-pathogenic strains of *Pseudomonas (P.) fluorescens* Pf0-1 engineered
252 with the type-III secretion system from *P. syringae* pv. *tomato (Pst)* DC3000
253 strain that are expressing effectors PopP2, mutant PopP2_{C321A}, AvrRps4,
254 mutant AvrRps4_{KRVY-AAAA}, AvrRpt2, and empty vector, respectively (Sohn *et al.*,
255 2009; Thomas *et al.*, 2009; Saucet *et al.*, 2015). This enabled the assessment
256 of HR activated by individual effector with their corresponding NLR proteins
257 without artefactual tissue damage from the carrier. Ws-2 ecotype containing
258 RRS1-R recognizes wild-type PopP2 (PopP2_{WT}), whereas RRS1-S-containing
259 Col-0 ecotype show no HR with PopP2_{WT} (Fig 1). Mutant PopP2 (PopP2_{C321}),
260 mutant AvrRps4 (AvrRps4_{KRVY-AAAA}) and empty vector served as non-
261 recognition negative controls which does not activate HR (Fig 1). AvrRpt2 is
262 known to be recognized by CC-NLR RPS2 (Axtell and Staskawicz, 2003;
263 Mackey *et al.*, 2003), and therefore HR was observed in all tested lines. We
264 found that only simultaneously over-expressing *RRS1-R* and *RPS4* can lead to
265 the gain-of-recognition of PopP2 in the susceptible ecotype Col-0 (Fig 1). No
266 HR was observed in *rps4-2 rps4b-2* double mutant when infiltrated with Pf0-
267 1:AvrRps4 (Fig 1). Thus, we propose that a balanced protein expression of
268 RRS1 and RPS4 is required for both suppressing autoimmunity and functional
269 recognition of the corresponding effectors.

270

271 **A survey of leaf-expressed genes reveals promoters for moderate and**
272 **balanced expression levels of RRS1 and RPS4**

273 Genome-wide expression profiling has revealed numerous genes altered by
274 PTI alone or PTI plus ETI at early time points of RRS1/RPS4-mediated immune
275 activation (Sohn *et al.*, 2014). This analysis also enabled the discovery of genes
276 that are moderately and constitutively expressed without changing their
277 transcript abundance during immune activation. In plants, gene expression
278 patterns and levels are usually specified by their promoters. Based on the
279 endogenous expression relative transcript abundance in the 'stable gene set',
280 we selected six promoters with 'moderate' expression (Table S1). We define
281 the 'moderate' expression based on two criteria: (1) the gene transcript
282 abundance with those promoters are at least 100 times more than the
283 endogenous transcript abundance of *RRS1* and *RPS4*; (2) the gene transcript
284 abundance with those promoters is lower than that with the 35S promoter. The
285 selected genes encode proteins that are involved in essential biological
286 processes that we expect to be expressed in most mesophyll cells, including a
287 delta-tonoplast intrinsic protein (our name; At1, locus identifier AT3G16240,
288 protein symbol name TIP2-1), a ribosomal protein S16 (At2, AT4G34620,
289 RPS16-1), a cysteine synthase isomer CysC1 (At3, AT3G61440, CYSC1), a
290 photosystem II subunit Q (At4, AT4G21280, PSBQ1), a xyloglucan
291 endotransglucosylase/hydrolase 6 (At5, AT5G65730, XTH6), and a ubiquitin-
292 like protein 5 (At6, AT5G42300, UBL5) (Table S1).

293 To test the strength of the selected Arabidopsis promoters (pAt1-pAt6) for
294 driving gene expression *in planta*, constructs were designed and generated to
295 express β -glucuronidase (GUS) (pAt:GUS). *Agrobacterium* strains carrying
296 each pAt:GUS construct was infiltrated in *Nicotiana (N.) benthamiana* leaves
297 with the infiltration buffer as negative control and GUS expressed under the
298 CaMV 35S promoter (35S:GUS) as positive control. GUS expressed under
299 pAt4 shows similar level of activity to that with 35S, whereas GUS activities
300 detected from other pAt promoters are significantly weaker (Fig S1).

301

302 **A T-DNA construct expresses RPS4, RRS1 and inducible AvrRps4**

303 We designed a binary vector to reconstruct the effector ligand AvrRps4 and its
304 receptors RRS1 and RPS4, using the Golden Gate Modular Cloning Toolbox

305 (Fig 2A) (Engler *et al.*, 2014). We chose moderate and balanced promoters
306 pAt2 and pAt3 from our promoter survey experiment for expressing RRS1 and
307 RPS4, respectively. We have also cloned *RRS1-R* full-length coding
308 sequences (CDS) from Ws-2 and *RPS4* full-length CDS from Col-0 for the
309 expression of RRS1-R and RPS4 proteins. We chose synthetic C-terminal-
310 fusion epitope tags His₆-TEV-FLAG₃ (HF) and HA₆ for detecting RRS1 and
311 RPS4 protein expressions, respectively (Fig 2A, Table S2) (Gauss *et al.*, 2005;
312 Soleimani *et al.*, 2013). We have used an E2-inducible system for AvrRps4
313 expression (Zuo *et al.*, 2000). We named this multi-gene stacking binary
314 construct 'Super ETI', or SETI. We have also generated constructs inducing
315 mutant AvrRps4^{KRVY-AAAA} or mutant AvrRps4^{E187A} as negative controls, and
316 named them SETI_KRVYmut and SETI_E187A, respectively. SETI_KRVYmut
317 and SETI_E187A can induce the expression of mutant AvrRps4 alleles, but no
318 induction of immunity because these two mutant AvrRps4 alleles cannot be
319 recognized by RRS1 and RPS4 (Sohn *et al.*, 2009, 2014). All restriction enzyme
320 sites for Bsal and Bpil in modules for promoters, CDSs for genes or epitope
321 tags and the terminators were synonymously eliminated (Fig 2A, Table S4).
322 More detailed information for the cloning can be found in supplemental
323 materials. To verify the SETI construct, we used a transient expression system
324 in *N. benthamiana* by infiltrating Agrobacteria that deliver the SETI T-DNA.
325 Protein accumulation of RRS1-R-HF and RPS4-HA was detected (Fig S2).

326

327 **The single-locus lines carrying the SETI T-DNA show inducible growth** 328 **arrest**

329 We generated transgenic Arabidopsis lines using the SETI, SETI_KRVYmut
330 and SETI_E187A construct expressing AvrRps4 (SETI_WT), AvrRps4^{KRVY-AAAA},
331 and AvrRps4^{E187A}, respectively. With the FastRed selection module, we have
332 selected approximately 20 positive SETI_WT T1 lines. The seedlings from the
333 T2 generation of 3 T1 lines were further tested for response to E2 treatment
334 (see Materials and Methods, Table S2). On E2-containing growth medium,
335 SETI_WT transgenic lines display severe growth arrest (Fig S3). We selected
336 one of the lines (T1-#8_T2-#4; SETI_WT) for subsequent experiments (Fig 2C,
337 Fig S3). We confirmed the protein expression of RRS1-R-HF and RPS4-HA
338 (Fig 2B). We also tested the expression of inducible AvrRps4-mNeon under

339 fluorescence microscope upon the treatment with E2. mNeonGreen signal was
340 detected at 24 hours post spray on transgenic seedlings, consistent with the
341 mRNA accumulation of *AvrRps4* at 4 hours post E2-infiltration in leaves (Fig
342 2D, Fig S2C).

343

344 **RRS1-R and RPS4 form pre-activation complexes in Arabidopsis**

345 The SETI lines enable detection of epitope-tagged RRS1-R and RPS4 (Fig 2B).
346 We investigated *in vivo* interaction of tagged RRS1-R and RPS4 by co-
347 immunoprecipitation (co-IP) with SETI_WT and SETI_E187A seedling extracts
348 with or without E2 induction. When RPS4-HA was immunoprecipitated using
349 HA beads, we found RRS1-R and RPS4 stay in association with each other
350 both before and 3 hours after the induction of *AvrRps4* expression (Fig 3).
351 There were no significant differences of RRS1-R and RPS4 association upon
352 *AvrRps4* induction. Induction of *AvrRps4* E187A also had no effect on RRS1-R
353 and RPS4 association. While all previous studies in interactions of RRS1-R and
354 RPS4 was tested only using *N. benthamiana* transient expression system (Huh
355 *et al.*, 2017), generation of SETI line enabled the detection of RRS1-R and
356 RPS4 interaction in its native system in Arabidopsis.

357

358 **Some but not all defence responses are induced by E2 in SETI lines**

359 The induced expression of multiple effectors, such as *AvrRpt2*, *AvrRpm1* and
360 *ATR13* can induce cell death or named macroscopic HR in Arabidopsis leaves
361 (McNellis *et al.*, 1998; Tornero *et al.*, 2002; Allen *et al.*, 2004). We therefore
362 tested whether induced expression of *AvrRps4* can trigger macroscopic HR in
363 Arabidopsis. We used SETI_eds1 as control, in which SETI_WT was crossed
364 with the mutant *eds1*. EDS1 is downstream genetic component of TIR-NLR-
365 mediated ETI (Aarts *et al.*, 1998; Falk *et al.*, 1999). As seen in Fig 4A, no HR
366 can be observed after *AvrRps4* expression is induced in the SETI leaves.
367 However, only the expression of *AvrRps4* but not *AvrRps4_KRVYmut* leads to
368 electrolyte leakage (Fig 4C). We also observed slightly stronger trypan blue
369 stains in the SETI leaves treated with E2 compared to mock treatment;
370 suggesting that the expression of *AvrRps4* causes microscopic or weak but not
371 macroscopic or strong HR in contrast to other known inducible effector lines
372 (Fig 4B).

373 Salicylic acid induction is another hallmark of ETI (Castel *et al.*, 2019). Enzymes
374 such as Isochorismate Synthase 1 (ICS1), Enhanced Disease Susceptibility 5
375 (EDS5) and AvrPphB Susceptible 3 (PBS3) are involved in the biosynthesis of
376 salicylic acid and the expression of these genes is also highly induced during
377 ETI (Sohn *et al.*, 2014). The expression of *ICS1* after the *AvrRps4* induction
378 was tested by quantitative real-time PCR. *ICS1* was highly induced 4 hours
379 after the induction of *AvrRps4* by E2 but not in the negative controls of
380 SETI_KRVYmut or SETI_eds1 (Fig 5A). In contrast, *Pathogenesis-Related*
381 *protein 1 (PR1)* was highly induced only 8 hours after the induction of *AvrRps4*
382 (Fig 5B). This shows that ETI triggered by RRS1/RPS4 is sufficient for the
383 induction of *ICS1* and the biosynthesis of salicylic acid, which subsequently
384 leads to expression of *PR1*.

385 Activation of mitogen-activated protein kinases (MAPKs) by PTI has been
386 reported under many cases and happens within a few minutes of the activation
387 of PTI. However, the activation of MAPKs by ETI is slower and lasts longer than
388 PTI-induced MAPK activation (Tsuda *et al.* 2013). We tested whether the
389 induced expression of *AvrRps4* can lead to MAPK activation in SETI_WT and
390 control lines Col-0, SETI_KRVYmut, and SETI_eds1. Treatment of flg22 for 10
391 minutes triggered phosphorylation of MAP kinases (Fig 5C). However, in
392 contrast to *AvrRpt2*-inducible transgenic Arabidopsis plants (Tsuda *et al.* 2013),
393 induced expression of *AvrRps4* does not activate MAPKs (Fig 5C).

394 We further tested if the induction of ETI would elevate resistance. We infiltrated
395 the leaves with E2 or mock solution one day before we infiltrated plants with
396 *Pst* DC3000 (see Materials and Methods). SETI_WT plants pre-treated with E2
397 are more resistant to the bacteria than those pre-treated with mock, while there
398 was no significant difference between E2 and mock pre-treatment in Col-0 (Fig
399 6).

400

401 Discussion

402 To facilitate studying the functional complex of RRS1 and RPS4 *in vivo*, we
403 generated an expression construct of E2-inducible *AvrRps4* stacked with
404 epitope-tagged RRS1 and RPS4. To achieve balanced expression levels
405 higher than endogenous expression of *RRS1* and *RPS4*, we surveyed
406 constitutively expressed gene promoters. Here, we report 6 new and tested

407 promoter modules that are compatible with the Golden Gate Modular Cloning
408 toolkit. We used two of the promoters to express *RRS1* and *RPS4*, and we
409 avoided autoimmunity induced by excessive expression of *RPS4* or non-
410 recognition of PopP2 cause by excessive expression of *RRS1-R*. We were also
411 able to generate inducible AvrRps4 expression to activate RRS1/RPS4-
412 mediated ETI under the control of E2 treatment. We thus were able to stack
413 genes for inducible expression of a pathogen effector and its NLR receptors in
414 one construct. In addition, with the epitope tags, we are able to monitor effector-
415 dependent changes in the NLR proteins without interference from using a
416 pathogen effector-delivery system. We could thus express any effectors or
417 pathogen ligands that will trigger immunity in plant cells with the E2-inducible
418 module, and their immune receptors using the same gene stacking strategy.
419 There are multiple advantages to enabling investigation of ETI without the
420 complication of co-activating PTI. Firstly, we could test the contribution of other
421 genes to ETI activation by introducing mutants into the SETI background, either
422 using conventional crossing or using genome-editing such as CRISPR/Cas9.
423 These lines can also help investigating downstream signalling from plant NLRs.
424 Multiple forward genetic screens have been conducted, but few novel
425 components have been found, and most mutations are either in the NLRs or
426 regulatory elements rather than signalling components (van Wersch *et al.*,
427 2016). Another plausible explanation is that the signalling path downstream of
428 plants NLRs is very short, but this is debatable, because several significant
429 steps are required for immunity. EDS1, PAD4 and SAG101 are required for
430 TIR-NLR signalling (Falk *et al.*, 1999; Gantner *et al.*, 2019). NRC family proteins
431 in Solanaceae species required for many NLRs, and NRG1/ADR1s in
432 Arabidopsis required for TIR-NLRs and ADR1s for some CC-NLRs (Bonardi *et al.*,
433 2011; Dong *et al.*, 2016; Wu *et al.*, 2017, 2019; Castel *et al.*, 2019). NRG1s
434 and ADR1s seem to function downstream of EDS1 and may function distinctly
435 with SAG101 and PAD4, respectively (Lapin *et al.*, 2019). SETI lines carry
436 heterologously expressed RRS1-R/RPS4 and also endogenous RRS1-S/RPS4,
437 RRS1B/RPS4B, which together provide three redundant copies of NLR pairs
438 that can recognize AvrRps4. In theory, in an EMS-mutagenesis forward genetic
439 screen to identify suppressors of immunity induced by AvrRps4, there should
440 be a reduced background of mutations in the receptor(s), improving prospects

441 to reveal mutations in genes that are functionally important in NLR signalling
442 and regulation.

443 With SETI, we are able to assess pure ETI response mediated by the TIR-NLRs,
444 RRS1 and RPS4. E2 induction provoked rapid transcriptional changes in
445 activation of defence genes and also ion leakage. AvrRps4-induced ETI
446 enhanced resistance against bacterial pathogens. However, neither MAPK
447 activation nor macroscopic HR, in contrast to other inducible ETI examples
448 (Tornero *et al.*, 2002; Tsuda *et al.*, 2013). This indicates that outputs of plant
449 NLRs might differ. Both TIR and CC domains alone are sufficient to activate
450 plant immunity. However, whether they signal through similar or different
451 downstream components is still unknown.

452 In diverse multicellular eukaryotes, immune complexes are assembled into
453 oligomeric complexes to signal downstream. The mammalian inflammasome,
454 assembled in response to bacterial peptide recognition by NAIP proteins and
455 subsequent activation and binding of NLRC4 proteins, is a classic example
456 (Zhang *et al.*, 2015). The plant CC NLR ZAR1 forms an effector-dependent
457 resistosome, which is a pentamer of ZAR1 assembled together with cofactors
458 PBL2 and RKS1 (Wang *et al.*, 2019). The structure of TIR domains implies that
459 activation might require the disassociation of the RRS1 and RPS4 TIR domains
460 and the oligomerization of RPS4 TIR domains (Williams *et al.*, 2014). In SETI
461 lines, RRS1 and RPS4 form a pre-activation complex in the absence of
462 pathogen effector. However, co-IP data cannot distinguish the ratio of which
463 RRS1 and RPS4 bind to each other. It will be interesting to check via various
464 non-denaturing methods if RRS1-R and RPS4 form a dimer or a higher order
465 oligomerization *in vivo*, or whether there is a conformational change in complex
466 upon effector recognition. Furthermore, with the SETI lines generated in this
467 study, we can ask what other co-factors are required for the activation of RRS1-
468 R and RPS4 at native conditions.

469 The availability of SETI lines also will enable us to study how PTI and ETI
470 interact with each other, especially in the context of RRS1- and RPS4-mediated
471 immunity. Some models have been proposed in discussing on this topic (Tsuda
472 *et al.*, 2009; Cui *et al.*, 2015). From the zig-zag model, PTI and ETI holds in
473 different threshold on activating immunity (Jones and Dangl, 2006). With SETI
474 line, we could specifically ask how physically PTI and ETI can influence each

475 other. A lot of evidence shows that the PTI receptors PRRs usually have very
476 specific post-translational modification events at early time points, there is also
477 some evidence showing ETI can activate somewhat overlapping but different
478 PTMs on immune-related proteins (Withers and Dong, 2017; Kadota *et al.*,
479 2019). It will be interesting to know how the activation of RRS1/PRS4 leads to
480 the changes of PTMs and how those changes contribute to the robustness of
481 immunity. In addition, transcriptional changes are not the only process reported
482 as the early changes of ETI but also the changes in translations (Meteignier *et al.*,
483 2017; Yoo *et al.*, 2019). Both work using inducible AvrRpm1 or AvrRpt2
484 reveal interesting observations on trade-off between defence and growth, and
485 the specific regulatory element in the genome (Meteignier *et al.*, 2017; Yoo *et al.*,
486 2019). Both effectors are recognized by CC-type NLRs, so it will be
487 interesting to know what changes in translations will be induced by TIR-NLRs
488 using SETI line. One can also use proteomics tools to generate complex
489 information using inducible SETI to fish for ETI-specific interaction networks.
490 Recently it has been shown plant NLRs can also form higher order protein
491 complex, similar to inflammasome in mammalian immune system. However, it
492 is unknown if all plant NLRs form the same kind of complex or using the same
493 mechanism to activate defence. It was noted that NLRs have evolved to partner
494 with other NLRs to function genetically, but if this model is also true
495 biochemically is still unknown (Adachi *et al.*, 2019). Unlike ZAR1, RRS1 and
496 RPS4 requires each other to function, and they localized and function
497 exclusively in the nuclei but not the cell membrane, so it will be interesting to
498 compare them once the transmission electron cryomicroscopic (Cryo-EM)
499 structure of RRS1 and RPS4 complex is resolved. SETI line could be a very
500 good toolkit to make mutagenesis to verify the function based on the structural
501 information.

502 We have observed the activation of ETI alone in the absence of pathogens is
503 sufficient to prime the resistance against bacterial pathogens in *Arabidopsis*
504 (Fig 6). Previously, we have reported a group of upregulated genes at the early
505 time point of activation of RRS1-R/RPS4 are related to salicylic acid pathway,
506 so it will be interesting to know if the elevated or primed resistance against
507 bacteria induced in SETI lines are due to the activation of salicylate pathway
508 (Sohn *et al.*, 2014).

509 Another major question regarding the signalling pathways is that SAG101 and
510 PAD4 seems to be redundant but functionally equivalent to EDS1 (Wagner *et al.*
511 *et al.*, 2013; Lapin *et al.*, 2019). They also have been shown to be genetically
512 linked to helper NLRs NRG1s and/or ADR1s to function (Castel *et al.*, 2019;
513 Wu *et al.*, 2019). Using SETI line, one can test their function more specifically
514 in ETI in the absence of PTI and many other unwanted pathogen interferences.

515

516 **Acknowledgements**

517 We thank the Gatsby Foundation (United Kingdom) for funding to the JDGJ
518 laboratory. BN was supported by the Norwich Research Park (NRP)
519 Biosciences Doctoral Training Partnership (DTP) from the Biotechnology and
520 Biological Sciences Research Council (BBSRC) (grant agreement:
521 BB/M011216/1). HA were supported by European Research Council Advanced
522 Grant “ImmunitybyPairDesign” (grant agreement: 669926). PD acknowledges
523 support from the European Union’s Horizon 2020 Research and Innovation
524 Program under Marie Skłodowska-Curie Actions (grant agreement: 656243)
525 and a Future Leader Fellowship from BBSRC (grant agreement:
526 BB/R012172/1). AR acknowledge support from the EMBO Long Term
527 Fellowship (ALTF-842-2015). HB was supported by the NRP DTP funding from
528 BBSRC (grant agreement: BB/M011216/1). YM were supported by
529 Biotechnology and Biological Sciences Research Council (BBSRC) Grant
530 (grant agreement: BB/M008193/1). LT, MY and JDGJ were supported by the
531 Gatsby Foundation funding to the Sainsbury Laboratory.

532

533 **References**

534 **Aarts N, Metz M, Holub E, Staskawicz BJ, Daniels MJ, Parker JE.** 1998.
535 Different requirements for EDS1 and NDR1 by disease resistance genes
536 define at least two R gene-mediated signaling pathways in Arabidopsis.
537 Proceedings of the National Academy of Sciences of the United States of
538 America **95**, 10306–10311.

539 **Adachi H, Derevnina L, Kamoun S.** 2019. NLR singletons, pairs, and
540 networks: evolution, assembly, and regulation of the intracellular
541 immunoreceptor circuitry of plants. Current Opinion in Plant Biology **50**, 121–
542 131.

543 **Allen RL, Bittner-Eddy PD, Grenville-Briggs LJ, Meitz JC, Rehmany AP,**

- 544 **Rose LE, Beynon JL.** 2004. Host-parasite coevolutionary conflict between
545 Arabidopsis and downy mildew. *Science* **306**, 1957–1960.
- 546 **Axtell MJ, Staskawicz BJ.** 2003. Initiation of RPS2-specified disease
547 resistance in Arabidopsis is coupled to the AvrRpt2-directed elimination of
548 RIN4. *Cell* **112**, 369–377.
- 549 **Bonardi V, Tang S, Stallmann A, Roberts M, Cherkis K, Dangl JL.** 2011.
550 Expanded functions for a family of plant intracellular immune receptors
551 beyond specific recognition of pathogen effectors. *Proceedings of the National*
552 *Academy of Sciences of the United States of America* **108**, 16463–16468.
- 553 **Castel B, Ngou P-M, Cevik V, Redkar A, Kim D-S, Yang Y, Ding P, Jones**
554 **JDG.** 2019. Diverse NLR immune receptors activate defence via the RPW8-
555 NLR NRG1. *The New Phytologist* **222**, 966–980.
- 556 **Cui H, Tsuda K, Parker JE.** 2015. Effector-triggered immunity: from
557 pathogen perception to robust defense. *Annual review of plant biology* **66**,
558 487–511.
- 559 **Dong OX, Tong M, Bonardi V, El Kasmi F, Woloshen V, Wunsch LK,**
560 **Dangl JL, Li X.** 2016. TNL-mediated immunity in Arabidopsis requires
561 complex regulation of the redundant ADR1 gene family. *The New Phytologist*
562 **210**, 960–973.
- 563 **Engler C, Youles M, Gruetzner R, Ehnert T-M, Werner S, Jones JDG,**
564 **Patron NJ, Marillonnet S.** 2014. A golden gate modular cloning toolbox for
565 plants. *ACS synthetic biology* [electronic resource] **3**, 839–843.
- 566 **Falk A, Feys BJ, Frost LN, Jones JD, Daniels MJ, Parker JE.** 1999. EDS1,
567 an essential component of R gene-mediated disease resistance in
568 Arabidopsis has homology to eukaryotic lipases. *Proceedings of the National*
569 *Academy of Sciences of the United States of America* **96**, 3292–3297.
- 570 **Gantner J, Ordon J, Kretschmer C, Guerois R, Stuttmann J.** 2019. An
571 EDS1-SAG101 Complex is Essential for TNL-mediated Immunity in *Nicotiana*
572 *benthamiana*. *The Plant Cell*.
- 573 **Gauss R, Trautwein M, Sommer T, Spang A.** 2005. New modules for the
574 repeated internal and N-terminal epitope tagging of genes in *Saccharomyces*
575 *cerevisiae*. *Yeast* **22**, 1–12.
- 576 **Heidrich K, Tsuda K, Blanvillain-Baufumé S, Wirthmueller L, Bautor J,**
577 **Parker JE.** 2013. Arabidopsis TNL-WRKY domain receptor RRS1 contributes
578 to temperature-conditioned RPS4 auto-immunity. *Frontiers in plant science* **4**,
579 403.
- 580 **Huh SU, Cevik V, Ding P, Duxbury Z, Ma Y, Tomlinson L, Sarris PF,**
581 **Jones JDG.** 2017. Protein-protein interactions in the RPS4/RRS1 immune
582 receptor complex. *PLoS Pathogens* **13**, e1006376.
- 583 **Jones JDG, Dangl JL.** 2006. The plant immune system. *Nature* **444**, 323–

584 329.

585 **Kadota Y, Liebrand TWH, Goto Y, et al.** 2019. Quantitative
586 phosphoproteomic analysis reveals common regulatory mechanisms between
587 effector- and PAMP-triggered immunity in plants. *The New Phytologist* **221**,
588 2160–2175.

589 **Lapin D, Kovacova V, Sun X, et al.** 2019. A coevolved EDS1-SAG101-
590 NRG1 module mediates cell death signaling by TIR-domain immune
591 receptors. *BioRxiv*.

592 **Livak KJ, Schmittgen TD.** 2001. Analysis of relative gene expression data
593 using real-time quantitative PCR and the 2(-Delta Delta C(T)) Method.
594 *Methods* **25**, 402–408.

595 **Mackey D, Belkadir Y, Alonso JM, Ecker JR, Dangl JL.** 2003. Arabidopsis
596 RIN4 is a target of the type III virulence effector AvrRpt2 and modulates
597 RPS2-mediated resistance. *Cell* **112**, 379–389.

598 **McNellis TW, Mudgett MB, Li K, Aoyama T, Horvath D, Chua NH,**
599 **Staskawicz BJ.** 1998. Glucocorticoid-inducible expression of a bacterial
600 avirulence gene in transgenic Arabidopsis induces hypersensitive cell death.
601 *The Plant Journal: for Cell and Molecular Biology* **14**, 247–257.

602 **Meteignier L-V, El Oirdi M, Cohen M, Barff T, Matteau D, Lucier J-F,**
603 **Rodrigue S, Jacques P-E, Yoshioka K, Moffett P.** 2017. Translatome
604 analysis of an NB-LRR immune response identifies important contributors to
605 plant immunity in Arabidopsis. *Journal of Experimental Botany* **68**, 2333–
606 2344.

607 **Narusaka M, Shirasu K, Noutoshi Y, Kubo Y, Shiraishi T, Iwabuchi M,**
608 **Narusaka Y.** 2009. RRS1 and RPS4 provide a dual Resistance-gene system
609 against fungal and bacterial pathogens. *The Plant Journal: for Cell and*
610 *Molecular Biology* **60**, 218–226.

611 **Porter K, Shimono M, Tian M, Day B.** 2012. Arabidopsis Actin-
612 Depolymerizing Factor-4 links pathogen perception, defense activation and
613 transcription to cytoskeletal dynamics. *PLoS Pathogens* **8**, e1003006.

614 **Sarris PF, Duxbury Z, Huh SU, et al.** 2015. A Plant Immune Receptor
615 Detects Pathogen Effectors that Target WRKY Transcription Factors. *Cell*
616 **161**, 1089–1100.

617 **Saucet SB, Ma Y, Sarris PF, Furzer OJ, Sohn KH, Jones JDG.** 2015. Two
618 linked pairs of Arabidopsis TNL resistance genes independently confer
619 recognition of bacterial effector AvrRps4. *Nature Communications* **6**, 6338.

620 **Schindelin J, Arganda-Carreras I, Frise E, et al.** 2012. Fiji: an open-source
621 platform for biological-image analysis. *Nature Methods* **9**, 676–682.

622 **Shaner NC, Lambert GG, Chammas A, et al.** 2013. A bright monomeric
623 green fluorescent protein derived from Branchiostoma lanceolatum. *Nature*

- 624 **Methods** **10**, 407–409.
- 625 **Sohn KH, Hughes RK, Piquerez SJ, Jones JDG, Banfield MJ.** 2012.
 626 Distinct regions of the *Pseudomonas syringae* coiled-coil effector AvrRps4 are
 627 required for activation of immunity. *Proceedings of the National Academy of*
 628 *Sciences of the United States of America* **109**, 16371–16376.
- 629 **Sohn KH, Segonzac C, Rallapalli G, Sarris PF, Woo JY, Williams SJ,**
 630 **Newman TE, Paek KH, Kobe B, Jones JDG.** 2014. The nuclear immune
 631 receptor RPS4 is required for RRS1SLH1-dependent constitutive defense
 632 activation in *Arabidopsis thaliana*. *PLoS Genetics* **10**, e1004655.
- 633 **Sohn KH, Zhang Y, Jones JDG.** 2009. The *Pseudomonas syringae* effector
 634 protein, AvrRPS4, requires in planta processing and the KRVY domain to
 635 function. *The Plant Journal: for Cell and Molecular Biology* **57**, 1079–1091.
- 636 **Soleimani VD, Palidwor GA, Ramachandran P, Perkins TJ, Rudnicki MA.**
 637 2013. Chromatin tandem affinity purification sequencing. *Nature Protocols* **8**,
 638 1525–1534.
- 639 **Thomas WJ, Thireault CA, Kimbrel JA, Chang JH.** 2009. Recombineering
 640 and stable integration of the *Pseudomonas syringae* pv. *syringae* 61 hrp/hrc
 641 cluster into the genome of the soil bacterium *Pseudomonas fluorescens* Pf0-
 642 1. *The Plant Journal: for Cell and Molecular Biology* **60**, 919–928.
- 643 **Tornero P, Chao RA, Luthin WN, Goff SA, Dangl JL.** 2002. Large-scale
 644 structure-function analysis of the *Arabidopsis* RPM1 disease resistance
 645 protein. *The Plant Cell* **14**, 435–450.
- 646 **Tsuda K, Mine A, Bethke G, Igarashi D, Botanga CJ, Tsuda Y,**
 647 **Glazebrook J, Sato M, Katagiri F.** 2013. Dual regulation of gene expression
 648 mediated by extended MAPK activation and salicylic acid contributes to robust
 649 innate immunity in *Arabidopsis thaliana*. *PLoS Genetics* **9**, e1004015.
- 650 **Tsuda K, Sato M, Stoddard T, Glazebrook J, Katagiri F.** 2009. Network
 651 properties of robust immunity in plants. *PLoS Genetics* **5**, e1000772.
- 652 **Wagner S, Stuttmann J, Rietz S, Guerois R, Brunstein E, Bautor J,**
 653 **Niefind K, Parker JE.** 2013. Structural basis for signaling by exclusive EDS1
 654 heteromeric complexes with SAG101 or PAD4 in plant innate immunity. *Cell*
 655 *Host & Microbe* **14**, 619–630.
- 656 **Wang J, Hu M, Wang J, Qi J, Han Z, Wang G, Qi Y, Wang H-W, Zhou J-M,**
 657 **Chai J.** 2019. Reconstitution and structure of a plant NLR resistosome
 658 conferring immunity. *Science* **364**.
- 659 **van Wersch R, Li X, Zhang Y.** 2016. Mighty dwarfs: *arabidopsis* autoimmune
 660 mutants and their usages in genetic dissection of plant immunity. *Frontiers in*
 661 *plant science* **7**, 1717.
- 662 **Wickham H.** 2016. *ggplot2 - Elegant Graphics for Data Analysis* . New York,
 663 NY: Springer-Verlag New York.

- 664 **Williams SJ, Sohn KH, Wan L, *et al.*** 2014. Structural basis for assembly and
665 function of a heterodimeric plant immune receptor. *Science* **344**, 299–303.
- 666 **Withers J, Dong X.** 2017. Post-translational regulation of plant immunity.
667 *Current Opinion in Plant Biology* **38**, 124–132.
- 668 **Wu C-H, Abd-El-Haliem A, Bozkurt TO, Belhaj K, Terauchi R, Vossen JH,**
669 **Kamoun S.** 2017. NLR network mediates immunity to diverse plant
670 pathogens. *Proceedings of the National Academy of Sciences of the United*
671 *States of America* **114**, 8113–8118.
- 672 **Wu Z, Li M, Dong OX, Xia S, Liang W, Bao Y, Wasteneys G, Li X.** 2019.
673 Differential regulation of TNL-mediated immune signaling by redundant helper
674 CNLs. *The New Phytologist* **222**, 938–953.
- 675 **Yoo H, Greene GH, Yuan M, Xu G, Burton D, Liu L, Marqués J, Dong X.**
676 2019. Translational Regulation of Metabolic Dynamics during Effector-
677 Triggered Immunity. *Molecular Plant*.
- 678 **Zhang L, Chen S, Ruan J, *et al.*** 2015. Cryo-EM structure of the activated
679 NAIP2-NLRC4 inflammasome reveals nucleated polymerization. *Science* **350**,
680 404–409.
- 681 **Zhang Z-M, Ma K-W, Gao L, Hu Z, Schwizer S, Ma W, Song J.** 2017.
682 Mechanism of host substrate acetylation by a YopJ family effector. *Nature*
683 *Plants* **3**, 17115.
- 684 **Zuo J, Niu Q-W, Chua N-H.** 2000. An estrogen receptor-based transactivator
685 XVE mediates highly inducible gene expression in transgenic plants. *The*
686 *Plant Journal: for Cell and Molecular Biology* **24**, 265–273.

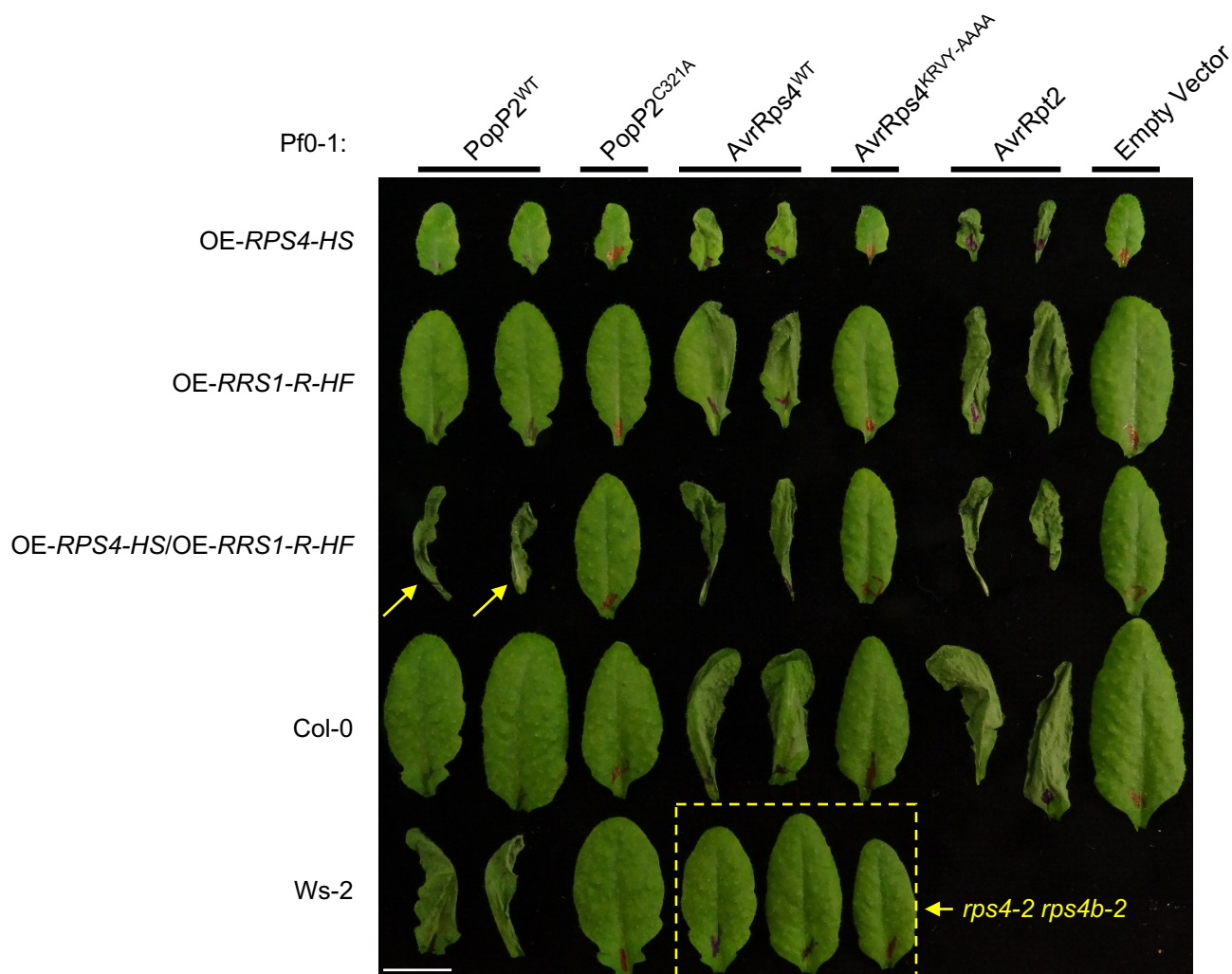


Fig. 1. Over-expression of RPS4 and RRS1-R reconstruct the recognition of PopP2 in Col-0. Arabidopsis transgenic lines overexpressing RPS4 (OE-*RPS4-HS*), RRS1-R (OE-*RRS1-R-HF*) or both generated by crossing (OE-*RPS4-HS/OE-RRS1-R-HF*) in the Col-0 background, with Col-0 and Ws-2 accession were tested for hypersensitive response (HR). 5-week old leaves were infiltrated with *Pseudomonas fluorescence* Pf0-1 strains carrying empty vector (EV), wild-type (WT) AvrRps4, mutant AvrRps4^{KRVY-AAAA}, WT PopP2, mutant PopP2^{C321A}, and WT AvrRpt2. Leaves were collected 1 day post infiltration (dpi) for imaging. Scale bar = 1cm. Yellow arrows indicate reconstructed PopP2 recognition of Col-0 background overexpressing RRS1-R and RPS4. Yellow dashed box highlights loss of AvrRps4 recognition in the double mutant *rps4-2 rps4b-2*. Infiltration of EV and AvrRpt2 serve as negative and positive controls of HR, respectively.

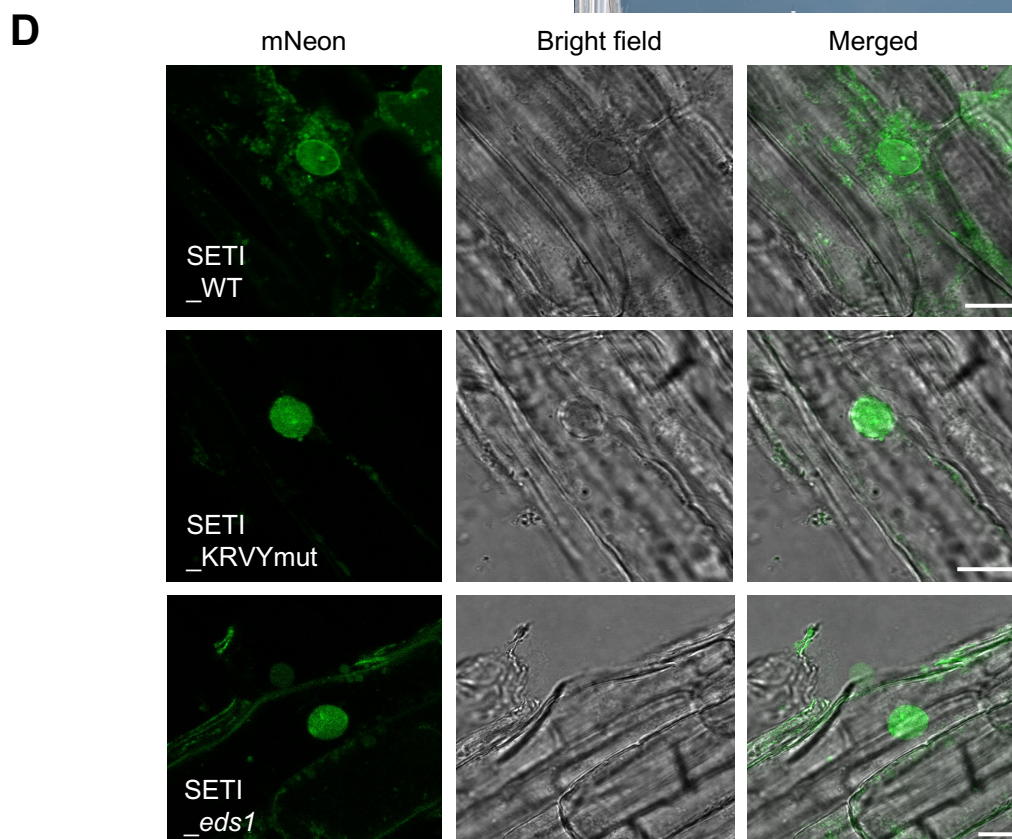
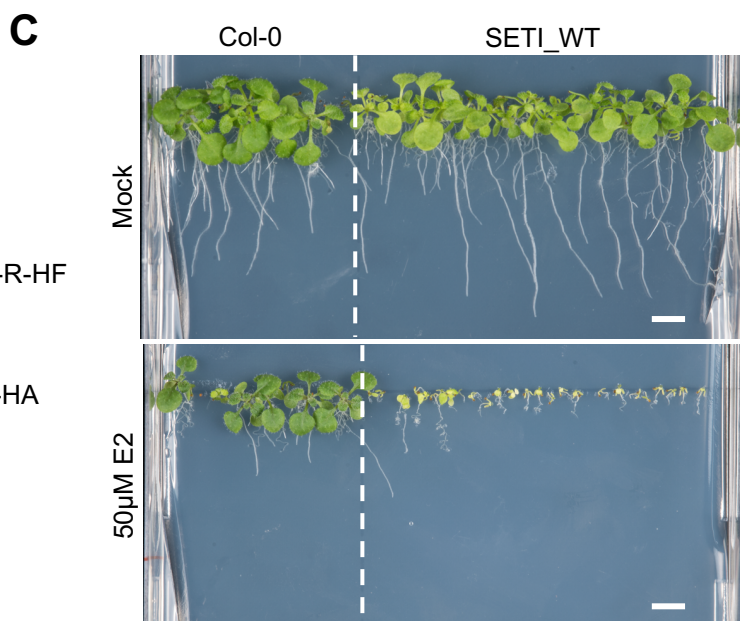
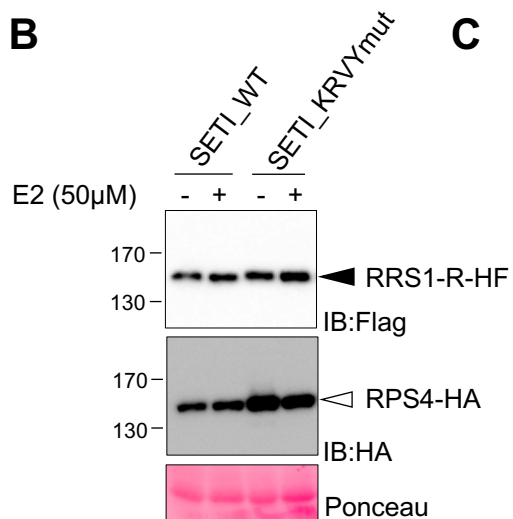
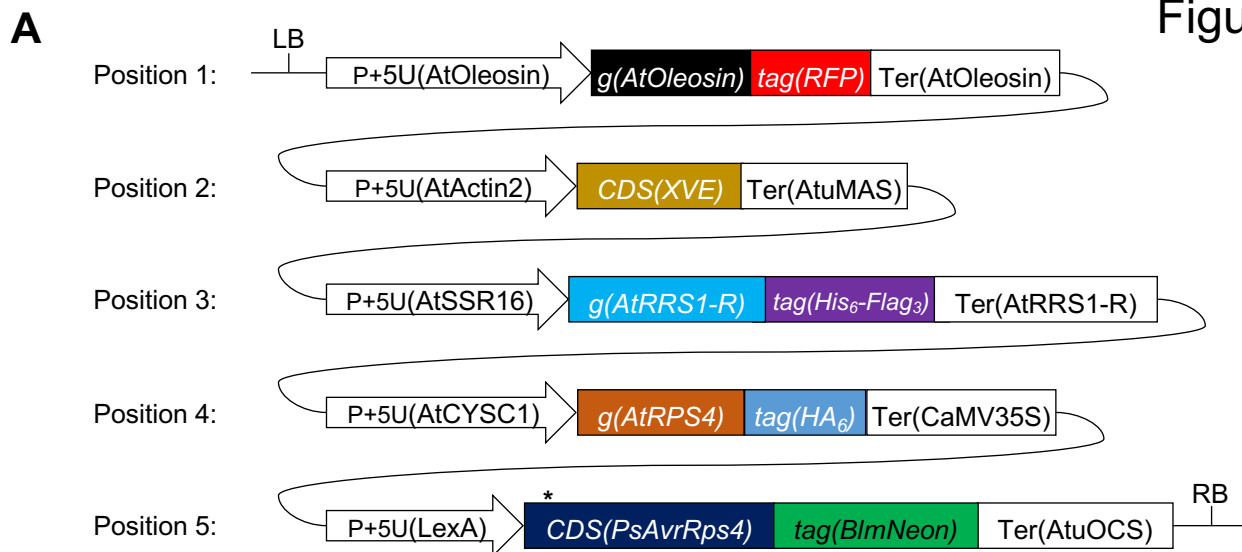


Fig 2. Single T-DNA expresses RRS1-R-HF, RPS4-HA and inducible wild-type AvrRps4 or AvrRps4 mutant variants

(A) Illustrative layout of the SUPER-ETI (SETI) construct. There are five individual expression units or Golden Gate Level 2 positional components listed, which are indicated position 1 to position 5. Position 1; expression unit of the FastRed selection marker (Shimada et al. 2010). Position 2, 5; chimeric transactivator XVE (LexA-VP16-ER) and the corresponding LexA inducible system to express AvrRps4 or its mutant variants under the control of β -estradiol (E2) treatment. Position 3, 4; full-length RRS1-R and RPS4 proteins with epitope tags His₆-Flag₃ and HA₆, respectively. All cloning details can be found in Methods and Materials. All individual units used for construct assembly can be found in the Supplemental Table 2 and 3.

(B) Protein accumulation of RRS1-R-HF (IB:Flag, black arrowhead) and RPS4-HA (IB:HA, white arrowhead) of SETI lines expressing AvrRps4 (SETI_WT) or mutant AvrRps4 KRVY-AAAA (SETI_KRVYmut). Seedlings were grown in liquid culture and induced with 50 μ M E2 for 2 hours at 7 days after germination (DAG). Ponceau staining of Rubisco large subunits were used as loading control.

(C) Seedling phenotype of SETI Arabidopsis transgenic line at 14 DAG in GM media containing Mock (0.1% DMSO) or 50 μ M E2. Col-0 was sown as control for the effect of E2 on seedling growth. Scale bar = 0.5cm

(D) Confocal images of SETI_WT, SETI_KRVYmut, SETI_eds1 root cells expressing AvrRps4-mNeon and AvrRps4^{KRVY-AAAA}-mNeon induced by 50 μ M E2 for 24h. mNeon channel shows nucleo-cytoplasmic localization of AvrRps4-mNeon and AvrRps4^{KRVY-AAAA}-mNeon. Bright field channel and merged image of mNeon and Bright field channel are shown together. Bars = 10 μ m.

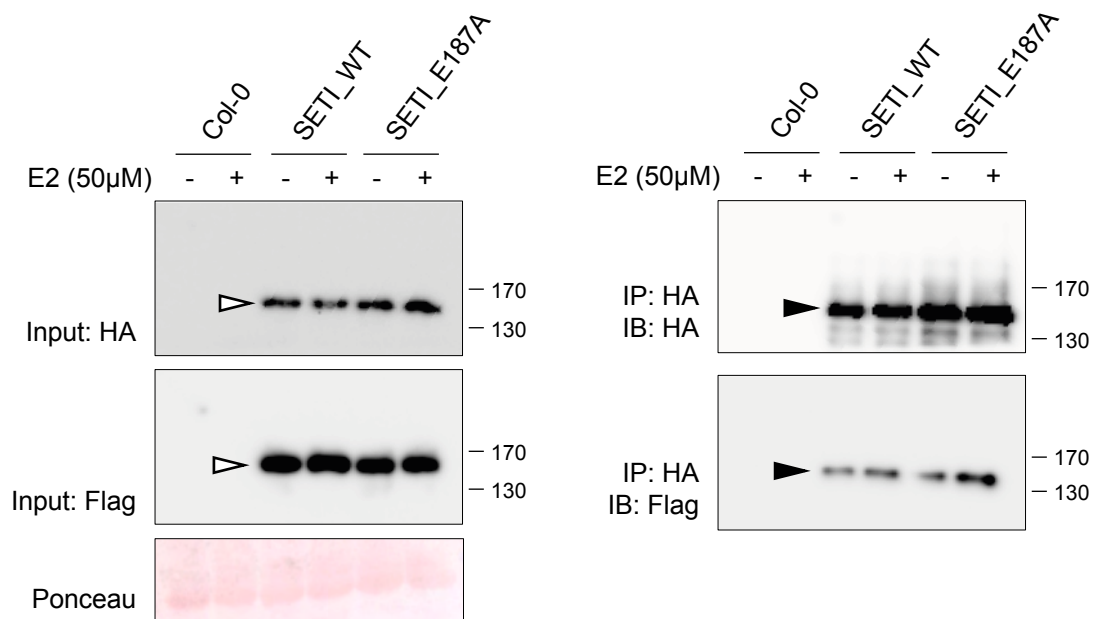


Fig 3. RRS1-R and RPS4 interact *in vivo*.

Co-immunoprecipitation of RRS1-R-HF with RPS4-HA. Col-0, SET1_WT, and SET1_E187A seedlings at DAG7 were treated with 50µM E2 for 3hours. Crude extracts were centrifuged and RPS4-HA proteins were immunoprecipitated with Anti-HA-conjugated beads. Immunoprecipitation of RPS4-HA, and co-immunoprecipitation of RRS1-R-HF were determined by immunoblot analysis with HA (IB:HA) or Flag (IB:Flag). Ponceau staining indicates equal loading of the input samples. RRS1-R-HF (black arrowhead), and RPS4-HA (white arrowhead) are indicated.

Figure 4

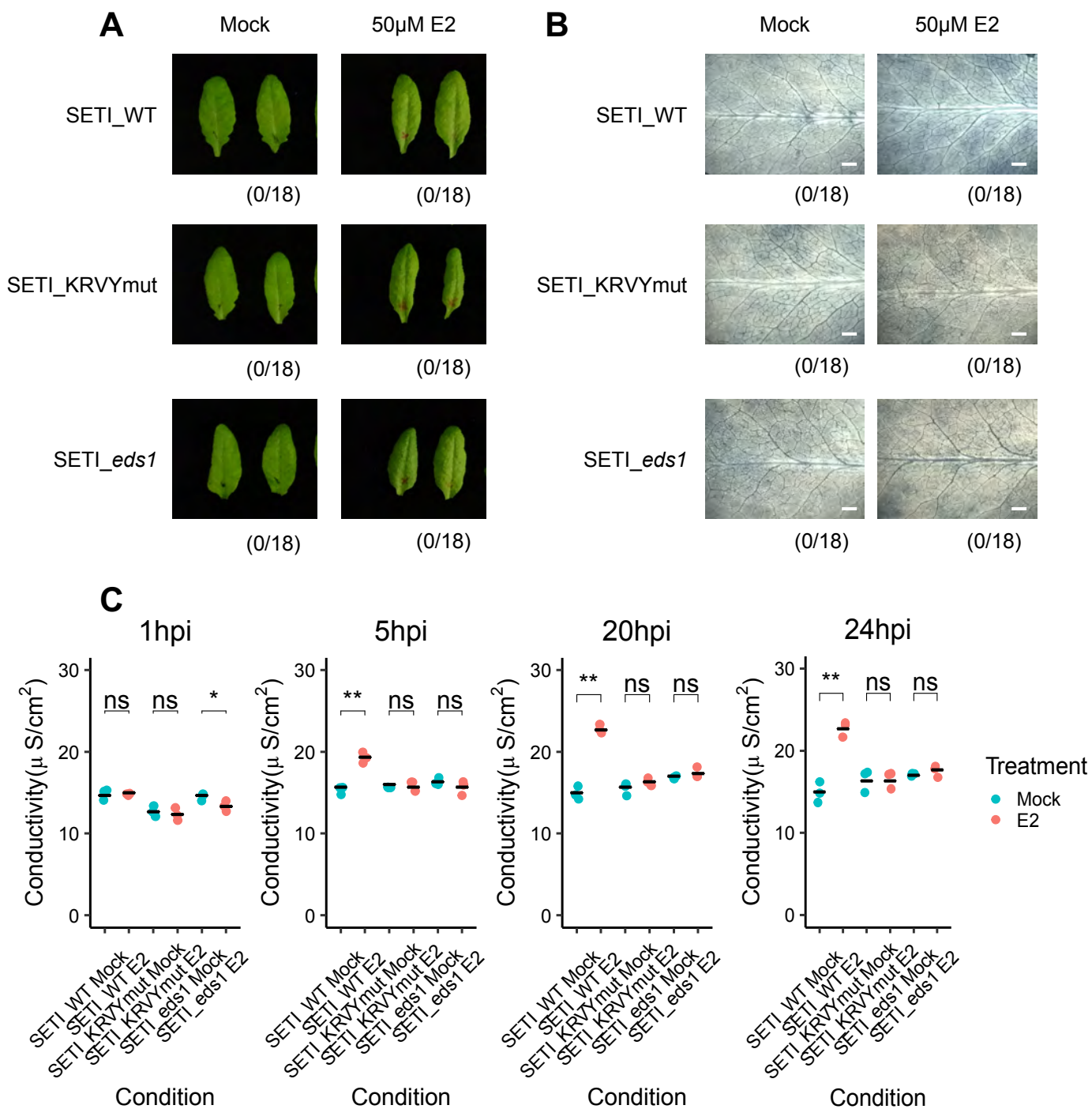


Fig. 4. Induced expression of AvrRps4 in *Arabidopsis* cause microscopic but not macroscopic cell death.

(A) HR phenotype assay in *Arabidopsis*. 5-week old SETI_WT, SETI_KRVYmut and SETI_eds1 leaves were infiltrated with Mock (1% DMSO) or 50 μ M E2. Images were taken at 1dpi. Numbers indicate the number of leaves displaying cell death from the total number of infiltrated leaves (18 for each genotype and treatment).

(B) Trypan blue staining. 5-week old SETI_WT, SETI_KRVYmut and SETI_eds1 were infiltrated with Mock (1% DMSO) or 50 μ M E2. Leaves were stained with trypan blue solution at 1dpi. After destaining, leaves were imaged using stereoscopic microscope. Scale bar = 0.5mm

(C) Electrolyte leakage assay. 5-week old SETI_WT, SETI_KRVYmut and SETI_eds1 leaves were infiltrated with Mock (1% DMSO) or 50 μ M E2. Fifteen leaf discs were collected for each data point. Conductivity was measured at 1, 5, 20 and 24 hours post infiltration (hpi). Each data point represents one technical replicate and three technical replicates are included per treatment and genotype for one biological replicate. Black line represents the mean of the technical replicates. This experiment was repeated three times independently with similar results (Supplemental Figure 2). Significant differences relative to the mock treatment in each genotype was calculated with t-test and the P-values are indicated as ns (non-significant), $P > 0.05$; *, $P < 0.05$; **, $P < 0.01$; ***, $P < 0.001$.

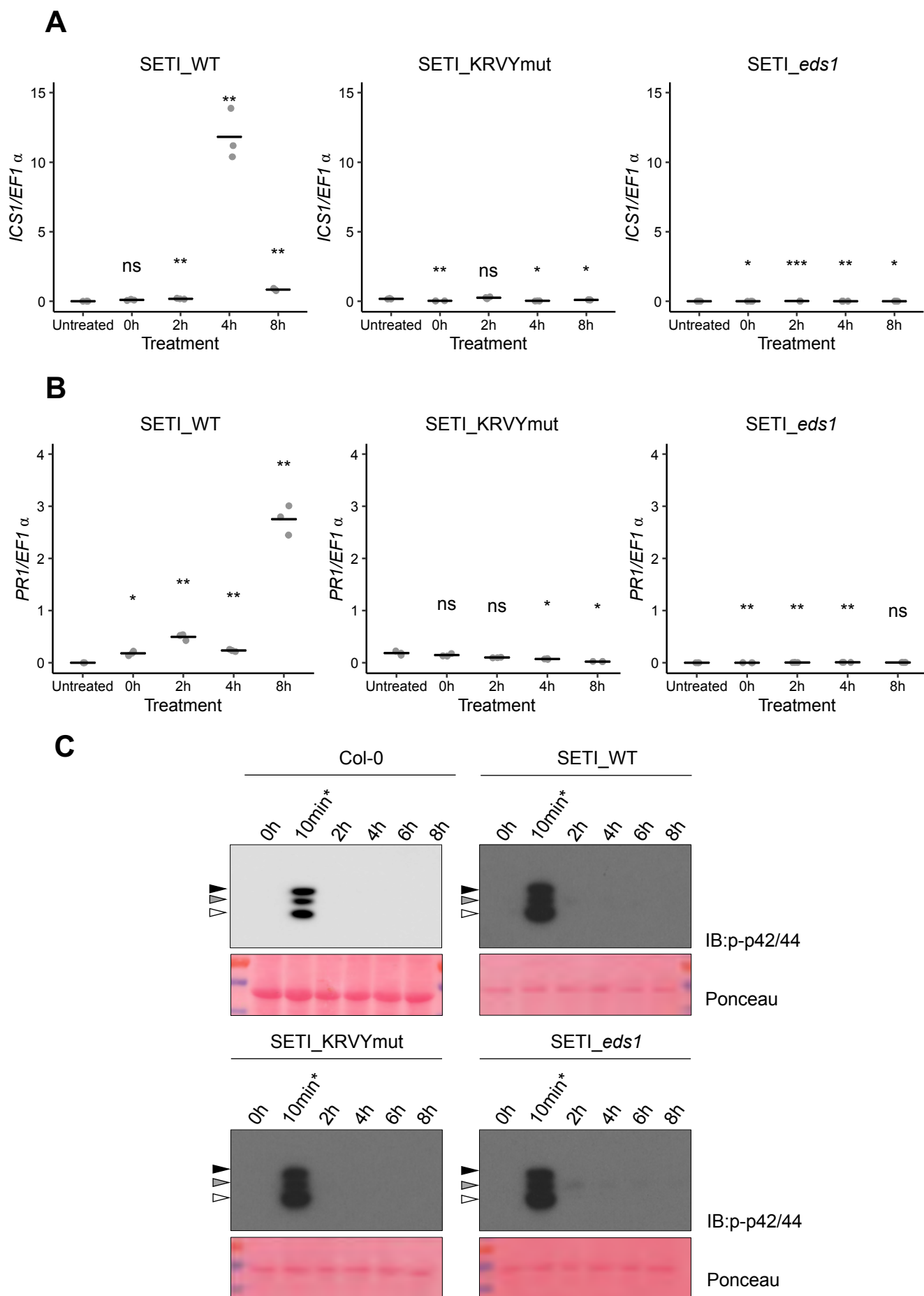


Fig. 5. Induced expression of AvrRps4 in *Arabidopsis* leads to *ICS1* and *PR1* expression, but not MAPK activation.

(A and B) *ICS1* (A) and *PR1* (B) expression after induction with E2 for 2, 4, and 8h in SETI (left panel), SETI_KRVYmut (middle panel) and SETI_eds1 (right panel) leaf samples. 5-week old SETI and SETI_KRVYmut leaves were infiltrated with 50 μ M E2. Samples were collected at 0, 2, 4 and 8hpi for RNA extraction and subsequent qPCR. Expression level is presented as relative to *EF1 α* expression. Each data point represents one technical replicate. Black line represents the mean of the technical replicates. This experiment was repeated three times independently with similar results. Significant differences relative to the untreated samples was calculated with t-test and the P-values are indicated as ns (non-significant), $P > 0.05$; *, $P < 0.05$; **, $P < 0.01$; ***, $P < 0.001$.

(C) Activation of MAP kinases in Col-0, SETI_WT, SETI_KRVYmut and SETI_eds1 seedlings by E2-induction of effector AvrRps4 or mutant AvrRps4^{KRVY-AAAA}. Seedlings grown in liquid culture at 7 dag were treated with 50 μ M E2 for indicated time points (0, 2, 4, 6, 8h) and collected for samples. Col-0, SETI_WT, SETI_KRVYmut and SETI_eds1 seedlings treated with 100nM flg22 for 10 minutes (10min*) were used as positive control. Proteins were extracted from these seedlings and phosphorylated MAP kinases were detected using p-p42/44 antibodies. Arrowheads indicate phosphorylated MAP kinases (black, pMPK6; grey, pMPK3; white, pMPK4/11). Ponceau staining were used as loading control.

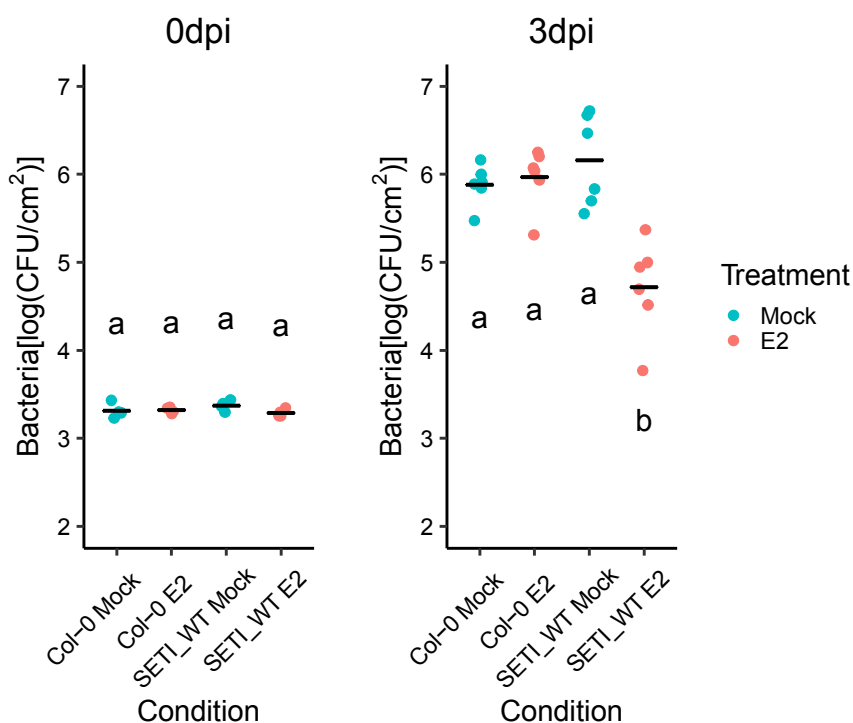


Fig. 6. Effector-triggered immunity triggered by the expression of AvrRps4 leads to resistance against *Pseudomonas syringae* pv. *tomato* strain DC3000.

5-week old SET1_WT and Col-0 leaves were infiltrated with Mock (1% DMSO) or 50 μ M E2. At 1dpi, leaves were inoculated with *Pst* DC3000 (OD₆₀₀=0.001). Bacteria in the leaves were then quantified as colony-forming units (CFU) at 0dpi and 3dpi. Each data point represents two leaves collected from one individual plant. Samples from four individual plants were collected for 0 dpi and samples from six individual plants were collected for 3 dpi. Black line represents the mean of the technical replicates. This experiment was repeated three times independently with similar results. Biological significance of the values were determined by one-way ANOVA followed by post hoc TukeyHSD analysis. Letters above the data points indicate significant differences (P<0.05).

Supplementary Table S1 Information of synthetic promoters used in this study.

Promoter Number	Promoter length (bp) ¹	Gene Symbol (UniProtKB)	AGI (TAIR)	Expression (TPM) ²
pAt1	1746	<i>TIP2-1</i>	AT3G16240	1600
pAt2	711	<i>RPS16-1</i>	AT4G34620	850
pAt3	550	<i>CYSC1</i>	AT3G61440	600
pAt4	348	<i>PSBQ1</i>	AT4G21280	557
pAt5	982	<i>XTH6</i>	AT5G65730	1000
pAt6	1659	<i>UBL5</i>	AT5G42300	280

1. The promoters are chosen from the first nucleotide next to the start codon ATG on the opposite direction of gene coding direction. The total length of each gene promoter is defined from the start codon of gene of interest up to either the 5' or 3' end of the immediate neighbouring gene.

2. TPM, tags per million. Transcripts of each gene under their endogenous promoters are indicated by the RNA sequencing profile data generated in Arabidopsis Ws-2 accession (Sohn *et al.*, 2013).

Supplementary Table S2 Golden Gate stacking construct of R genes and effector.

Position in Level2	Flank ¹	P+5U ²	CDS or genomic ³	cTag ⁴	Ter ⁵	Flank	Simplified Module
1	TGCC	AtOleosin ⁶	<i>AtOleosin</i>	<i>RFP</i>	AtOleosin	GCAA	FastRed
2	TTAC	AtActin2	XVE		AtuMas ⁷	CAGA	XVE
3	GCAA	AtSSR16 ⁸	<i>AtRRS1-R</i>	<i>Hellfire</i> ⁹	AtRRS1-R	ACTA	RRS1-R-HF
4	ACTA	AtCysC1 ¹⁰	<i>AtRPS4</i>	<i>HA</i> ₆ ¹¹	CaMV35S	TTAC	RPS4-HA
5	CAGA	LexA	<i>PsAvrRps4</i> ¹²	<i>BlmNeon</i> ¹³	AtuOcs ¹⁴	TGTG	LexA:AvrRps4-mNeon
End Linker	TGTG	gaggatgcacatgtgaccga				GGGA	pELE-5
Back Bone	TGCC	-				GGGA	pAGM4723

1. Flank: the flank sequences indicate the overhang sequence generated by the restriction enzyme Bpil from the level 1 modules to the level 2 destination backbone, before the final ligation reaction.

2. P+5U: promoter and 5' untranslated region (UTR).

3. CDS or genomic: coding sequence or full-length genomic sequence that includes potential introns.

4. cTag: c-terminal in-frame coding sequence for epitope tag.

5. Ter: terminator.

6. AtOleosin: AT4G25140, a protein found in oil bodies, involved in seed lipid accumulation, that is specifically expressed in seed coat.

7. AtuMas: terminator of Mas1 agropine synthesis reductase from *Agrobacterium tumefaciens* (Engler *et al.*, 2014).

8. AtSSR16: SMALL SUBUNIT RIBOSOMAL PROTEIN 16, AT4G34620; was named as pAt2 in our 'moderate promoter' database for intermediate expressing control in transgenic Arabidopsis leaves.

9. HellFire: His₆-TEV-FLAG₃, a tandem epitope tag with 6× histidine, TEV protease cleavage site and 3× FLAG tag (Soleimani *et al.*, 2013); here we simplify it as HF.

10. AtCYSC1: CYSTEINE SYNTHASE C1, AT3G61440, was named as pAt3 in our 'moderate promoter' database for intermediate expressing control in transgenic Arabidopsis leaves.

11. HA₆: a tag with 6 tandem HA repeats (Gauss *et al.*, 2005).

12. PsAvrRps4: effector protein AvrRps4 from *Pseudomonas syringae* pv. *psis*. Here this module can be placed with either wild-type or mutant AvrRps4 coding sequence.

13. BlmNeon: mNeonGreen protein, a bright monomeric green fluorescent protein derived from *Branchiostoma lanceolatum* (Shaner *et al.*, 2013).

14. AtuOcs: terminator of octopine synthase from *Agrobacterium tumefaciens* (Engler *et al.*, 2014).

Supplementary Table S3

Supplementary Table S3 Golden Gate cloning modules used in this work.

Modules for Cloning	TSL Synbio Name	Description of Inserts	Backbones	Overhangs for Ligation	
Level 1; Selection Cassettes	pICSL11015	See Table S2 FastRed module	pICH47732	TGCC	GCAA
Level 1; Inducible Cassettes	pICSL11037	See Table S2 XVE module	pICH47742	GCAA	ACTA
Level 0; Promoters + 5' Untranslated Regions (UTRs)	pICSL12028	AtSSR16 promoter, Col-0 allele	-	GGAG	AATG
Level 0; Coding Sequence (CDS) Without A Stop Codon	pICSL80072	<i>AtRRS1-R</i> CDS from genomic DNA, Ws-2 allele, BbsI and BpI sites are removed	-	AATG	TTCG
Level 0; C-terminal Tag	pICSL50001	Hellfire tag, His ₆ -TEV-FLAG ₃	-	TTCG	GCTT
Level 0; 3' UTRs and terminators	pICSL60019	AtRRS1-R terminator, Ws-2 allele	-	GCTT	CGCT
Level 0; Promoters + 5' UTRs	pICSL12007	AtCysC1 promoter, Col-0 allele	-	GGAG	AATG
Level 0; CDS Without A Stop Codon	pICSL80073	<i>AtRPS4</i> CDS from genomic DNA, Col-0 allele, BbsI and BpI sites are removed	-	AATG	TTCG
Level 0; C-terminal Tag	pICSL50009	Human influenza hemagglutinin tag, HA ₆	-	TTCG	GCTT
Level 0; 3' UTRs and terminators	pICH41414	CaMV 35S terminator	-	GCTT	CGCT
Level 0; Promoters + 5' UTRs	pICSL12005	LexA inducible promoter	-	GGAG	AATG
Level 0; CDS Without A Stop Codon	pICSL80070	AvrRps4 wild-type coding sequence (CDS) from <i>Pseudomonas syringae</i> , BbsI and BpI sites are removed	-	AATG	TTCG
Level 0; CDS Without A Stop Codon	pICSL80071	AvrRps4 CDS with KRVY135-138AAAA substitutions, BbsI and BpI sites are removed	-	AATG	TTCG
Level 0; CDS Without A Stop Codon	pICSL80074	AvrRps4 CDS with E187A substitution, BbsI and BpI sites are removed	-	AATG	TTCG
Level 0; C-terminal Tag	pICSL50015	mNeonGreen fluorescent protein from <i>Branchiostoma lanceolatum</i> , BbsI and BpI sites are removed	-	TTCG	GCTT
Level 1; Expression Cassettes	pICSL11162	See Table S2 RRS1-R-HF module	pICH47751	ACTA	TTAC
Level 1; Expression Cassettes	pICSL11163	See Table S2 RPS4-HA module	pICH47761	TTAC	CAGA
Level 1; Expression Cassettes	pICSL11164	See Table S2 LexA:AvrRps4-mNeon module	pICH47772	CAGA	TGTG
Level 1; Expression Cassettes	pICSL11165	Similar to pICSL11164, but with KRVY135-138AAAA substitutions	pICH47772	CAGA	TGTG
Level 1; Expression Cassettes	pICSL11166	Similar to pICSL11164, but with E187A substitution	pICH47772	CAGA	TGTG

Supplementary Table S4 Primers used in this study.

Primer Name	Directions	Nucleotide Sequence (5' to 3')
For real-time quantitative PCR		
AtEF1 α _RT_Fw	forward	CAGGCTGATTGTGCTGTTCTTA
AtEF1 α _RT_Rv	reverse	GTTGTATCCGACCTTCTTCAGG
AtICS1_RT_Fw	forward	CAATTGGCAGGGAGACTTACG
AtICS1_RT_Rv	reverse	GAGCTGATCTGATCCCGACTG
AtPR1_RT_Fw	forward	ATACACTCTGGTGGGCCTTACG
AtPR1_RT_Rv	reverse	TACACCTCACTTTGGCACATCC
AvrRps4_RT_Fw	forward	ATGACTCGAATTTCAACC
AvrRps4_RT_Rv	reverse	GGTCCACCCAATAGGGATTTGGGTG
For cloning		
AvrRps4_dom_Fw	forward	GAGGGTCTCAAATGACTCGAATTTCAACCAGTTCAG
AvrRps4_dom_Rv	reverse	GAGGGTCTCACGAACCTTGGTTGATTCTGCGGTCTCTCG
RPS4_dom_1_Fw	forward	agGAAGACAAAATGGAGACATCATCTATTTCCACTGTGGAgGAC
RPS4_dom_1_Rv	reverse	agGAAGACAAGTCcTCATAGTCGTCGATAAAGAC
RPS4_dom_2_Fw	forward	agGAAGACAAGGACAGAGGTCAACCTCTAGATG
RPS4_dom_2_Rv	reverse	agGAAGACAAGTtTTCACCGCCTTCACAATTTTATTG
RPS4_dom_3_Fw	forward	agGAAGACAAAaACAGCGTTGACCGGAATACCACCGG
RPS4_dom_3_Rv	reverse	agGAAGACAAAtACACTGACAATATTAGGGCTGG
RPS4_dom_4/5_Fw	forward	agGAAGACAAGtattccaagtgagttatgatgaattg
RPS4_dom_4/5_Rv	reverse	agGAAGACAACctccacttcagacaagtctagg
RPS4_dom_6_Fw	forward	agGAAGACAAGAgGACGAAACGAGCTTAGACCGCGACCAC
RPS4_dom_6_Rv	reverse	agGAAGACAATtTTCAGCGAACTACAGCCGTGTGCATCTAAGC
RPS4_dom_7_Fw	forward	agGAAGACAAAAaACAGTTTCAAAGCCTTTGGCCCGTA
RPS4_dom_7_Rv	reverse	agGAAGACAATaTCTTCATCTTTTACTTTAAAGGTG
RPS4_dom_8_Fw	forward	agGAAGACAAGAtAAGTCTTGGGTGCGCATATACTTGTCC
RPS4_dom_8_Rv	reverse	agGAAGACAAGAAAtACATGGTCTAGCTCAATCTTATCTTT
RPS4_dom_9_Fw	forward	agGAAGACAAaTTCATTGGATACACCAGTTG
RPS4_dom_9_Rv	reverse	agGAAGACAACgaaccGAAATTCTTAACCGTGTGCATGA

Supplementary Table S5 Statistical analysis results.

Figure 4C

Tukey multiple comparison of means

1hpi

Condition 1	Condition 2	Diff ¹	Lower ²	Upper ²	p adjusted ³
SETI_eds1 Mock	SETI_eds1 E2	-0.33333330	-3.07588100	2.40921400	0.99814890
SETI_KRVYmut E2	SETI_eds1 E2	-0.33333330	-3.07588100	2.40921400	0.99814890
SETI_KRVYmut Mock	SETI_eds1 E2	-0.66666670	-3.40921400	2.07588100	0.95879800
SETI_WT E2	SETI_eds1 E2	0.00000000	-2.74254700	2.74254700	1.00000000
SETI_WT Mock	SETI_eds1 E2	-1.00000000	-3.74254700	1.74254700	0.81720430
SETI_KRVYmut E2	SETI_eds1 Mock	0.00000000	-2.74254700	2.74254700	1.00000000
SETI_KRVYmut Mock	SETI_eds1 Mock	-0.33333330	-3.07588100	2.40921400	0.99814890
SETI_WT E2	SETI_eds1 Mock	-0.33333330	-3.07588100	2.40921400	0.99814890
SETI_WT Mock	SETI_eds1 Mock	-0.66666670	-3.40921400	2.07588100	0.95879800
SETI_KRVYmut Mock	SETI_KRVYmut E2	-0.33333330	-3.07588100	2.40921400	0.99814890
SETI_WT E2	SETI_KRVYmut E2	-0.33333330	-3.07588100	2.40921400	0.99814890
SETI_WT Mock	SETI_KRVYmut E2	-0.66666670	-3.40921400	2.07588100	0.95879800
SETI_WT E2	SETI_KRVYmut Mock	-0.66666670	-3.40921400	2.07588100	0.95879800
SETI_WT Mock	SETI_KRVYmut Mock	-0.33333330	-3.07588100	2.40921400	0.99814890
SETI_WT Mock	SETI_WT E2	-1.00000000	-3.74254700	1.74254700	0.81720430

5hpi

Condition 1	Condition 2	Diff	Lower	Upper	p adjusted
SETI_eds1 Mock	SETI_eds1 E2	-1.00000000	-8.05166000	6.05166000	0.99617570
SETI_KRVYmut E2	SETI_eds1 E2	-3.00000000	-10.05166000	4.05166000	0.71072430
SETI_KRVYmut Mock	SETI_eds1 E2	-3.33333330	-10.38499300	3.71832700	0.62047410
SETI_WT E2	SETI_eds1 E2	24.33333330	17.28167300	31.38499300	0.00000080
SETI_WT Mock	SETI_eds1 E2	2.33333330	-4.71832700	9.38499300	0.86763760
SETI_KRVYmut E2	SETI_eds1 Mock	-2.00000000	-9.05166000	5.05166000	0.92433520
SETI_KRVYmut Mock	SETI_eds1 Mock	-2.33333330	-9.38499300	4.71832700	0.86763760
SETI_WT E2	SETI_eds1 Mock	25.33333330	18.28167300	32.38499300	0.00000050
SETI_WT Mock	SETI_eds1 Mock	-3.33333330	-3.71832700	10.38499300	0.62047410
SETI_KRVYmut Mock	SETI_KRVYmut E2	-0.33333330	-7.38499300	6.71832700	0.99998160
SETI_WT E2	SETI_KRVYmut E2	27.33333330	20.28167300	34.38499300	0.00000020
SETI_WT Mock	SETI_KRVYmut E2	5.33333330	-1.71832700	12.38499300	0.18678740
SETI_WT E2	SETI_KRVYmut Mock	27.66666670	20.61500700	34.71832700	0.00000020
SETI_WT Mock	SETI_KRVYmut Mock	5.66666670	-1.38499300	12.71832700	0.14639040
SETI_WT Mock	SETI_WT E2	-22.00000000	-29.05166000	-14.94834000	0.00000250

20hpi

Condition 1	Condition 2	Diff	Lower	Upper	p adjusted
SETI_eds1 Mock	SETI_eds1 E2	-3.33333333	-12.656202	5.989535	0.8284027
SETI_KRVYmut E2	SETI_eds1 E2	-5.00000000	-14.322868	4.322868	0.4993132
SETI_KRVYmut Mock	SETI_eds1 E2	-5.33333333	-14.656202	3.989535	0.4350794
SETI_WT E2	SETI_eds1 E2	40.33333333	31.010465	49.656202	0.0000001
SETI_WT Mock	SETI_eds1 E2	-0.66666667	-9.989535	8.656202	0.9998581
SETI_KRVYmut E2	SETI_eds1 Mock	-1.66666667	-10.989535	7.656202	0.9889748
SETI_KRVYmut Mock	SETI_eds1 Mock	-2.00000000	-11.322868	7.322868	0.9755368
SETI_WT E2	SETI_eds1 Mock	43.66666667	34.343798	52.989535	0.0000000
SETI_WT Mock	SETI_eds1 Mock	2.66666667	-6.656202	11.989535	0.9218678
SETI_KRVYmut Mock	SETI_KRVYmut E2	-0.33333333	-9.656202	8.989535	0.9999954
SETI_WT E2	SETI_KRVYmut E2	45.33333333	36.010465	54.656202	0.0000000
SETI_WT Mock	SETI_KRVYmut E2	4.33333333	-4.989535	13.656202	0.6357179
SETI_WT E2	SETI_KRVYmut Mock	45.66666667	36.343798	54.989535	0.0000000
SETI_WT Mock	SETI_KRVYmut Mock	4.66666667	-4.656202	13.989535	0.5667788
SETI_WT Mock	SETI_WT E2	-41.00000000	-50.322868	-31.677132	0.0000001

24hpi

Condition 1	Condition 2	Diff	Lower	Upper	p adjusted
SETI_eds1 Mock	SETI_eds1 E2	-3.6666667	-13.298177	5.964843	0.7907177
SETI_KRVYmut E2	SETI_eds1 E2	-4.6666667	-14.298177	4.964843	0.5976463
SETI_KRVYmut Mock	SETI_eds1 E2	-5.6666667	-15.298177	3.964843	0.4072727
SETI_WT E2	SETI_eds1 E2	41.6666667	32.035157	51.298177	0.0000001
SETI_WT Mock	SETI_eds1 E2	-1.3333333	-10.964843	8.298177	0.9965824
SETI_KRVYmut E2	SETI_eds1 Mock	-1.00000000	-10.63151	8.63151	0.9991284
SETI_KRVYmut Mock	SETI_eds1 Mock	-2.00000000	-11.63151	7.63151	0.9787215
SETI_WT E2	SETI_eds1 Mock	45.3333333	35.701823	54.964843	0.0000000
SETI_WT Mock	SETI_eds1 Mock	2.3333333	-7.298177	11.964843	0.9593638
SETI_KRVYmut Mock	SETI_KRVYmut E2	-1.00000000	-10.63151	8.63151	0.9991284
SETI_WT E2	SETI_KRVYmut E2	46.3333333	36.701823	55.964843	0.0000000
SETI_WT Mock	SETI_KRVYmut E2	3.3333333	-6.298177	12.964843	0.8458559
SETI_WT E2	SETI_KRVYmut Mock	47.3333333	37.701823	56.964843	0.0000000
SETI_WT Mock	SETI_KRVYmut Mock	4.3333333	-5.298177	13.964843	0.664365
SETI_WT Mock	SETI_WT E2	-43.00000000	-52.63151	-33.36849	0.0000000

Supplementary Table S5 (cont.)

Figure 5A, B

PR1/EF1A in SET1_WT

Group 1	Group 2	p ⁴	p adjusted	p.format ⁵	p.signif ⁶	method
0h	Untreated	0.0173	0.035	0.0173	*	T-test
2h	Untreated	0.00493	0.028	0.0049	**	T-test
4h	Untreated	0.00258	0.026	0.0026	**	T-test
8h	Untreated	0.00352	0.028	0.0035	**	T-test

PR1/EF1A in SET1_KRVYmut

Group 1	Group 2	p	p adjusted	p.format	p.signif	method
0h	Untreated	0.248	0.25	0.24812	ns	T-test
2h	Untreated	0.062	0.19	0.06204	ns	T-test
4h	Untreated	0.0342	0.17	0.03423	*	T-test
8h	Untreated	0.0191	0.11	0.01912	*	T-test

ICS1/EF1A in SET1_WT

Group 1	Group 2	p	p adjusted	p.format	p.signif	method
0h	Untreated	0.075	0.11	0.07535	ns	T-test
2h	Untreated	0.0096	0.05	0.00969	**	T-test
4h	Untreated	0.00788	0.055	0.00788	**	T-test
8h	Untreated	0.00292	0.023	0.00292	**	T-test

ICS1/EF1A in SET1_KRVYmut

Group 1	Group 2	p	p adjusted	p.format	p.signif	method
0h	Untreated	0.00713	0.057	0.0071	**	T-test
2h	Untreated	0.182	0.36	0.1819	ns	T-test
4h	Untreated	0.0115	0.08	0.0115	*	T-test
8h	Untreated	0.0369	0.17	0.0369	*	T-test

Figure 6

0dpi

Tukey multiple comparison of means

Condition 1	Condition 2	Diff	Lower	Upper	p adjusted
Col-0 Mock	Col-0 E2	-0.009058683	-0.13119346	0.11307609	0.996022
SET1_WT E2	Col-0 E2	-0.031042838	-0.15317762	0.09109194	0.8730022
SET1_WT Mock	Col-0 E2	0.051462467	-0.07067231	0.17359724	0.6085929
SET1_WT E2	Col-0 Mock	-0.021984155	-0.14411893	0.10015062	0.9489591
SET1_WT Mock	Col-0 Mock	0.06052115	-0.06161363	0.18265593	0.4829018
SET1_WT Mock	SET1_WT E2	0.082505305	-0.03962947	0.20464008	0.2391907

T-test

Genotype	Group1	Group2	p	p.adj	p.format	p.signif
Col-0	Col-0 E2	Col-0 Mock	0.852	0.85	0.852	ns
SET1_WT	SET1_WT E2	SET1_WT Mock	0.0676	0.14	0.068	ns

3dpi

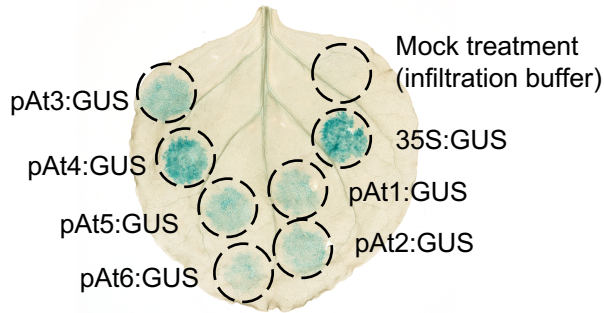
Tukey multiple comparison of means

Condition 1	Condition 2	Diff	Lower	Upper	p adjusted
Col-0 Mock	Col-0 E2	-0.08591854	-0.7827627	0.6109256	0.9854528
SET1_WT E2	Col-0 E2	-1.2506235	-1.9474676	-0.5537794	0.0003516
SET1_WT Mock	Col-0 E2	0.19040795	-0.5064362	0.8872521	0.8692549
SET1_WT E2	Col-0 Mock	-1.16470496	-1.8615491	-0.4678608	0.0007702
SET1_WT Mock	Col-0 Mock	0.27632649	-0.4205176	0.9731706	0.6877704
SET1_WT Mock	SET1_WT E2	1.44103146	0.7441873	2.1378756	0.0000637

T-test

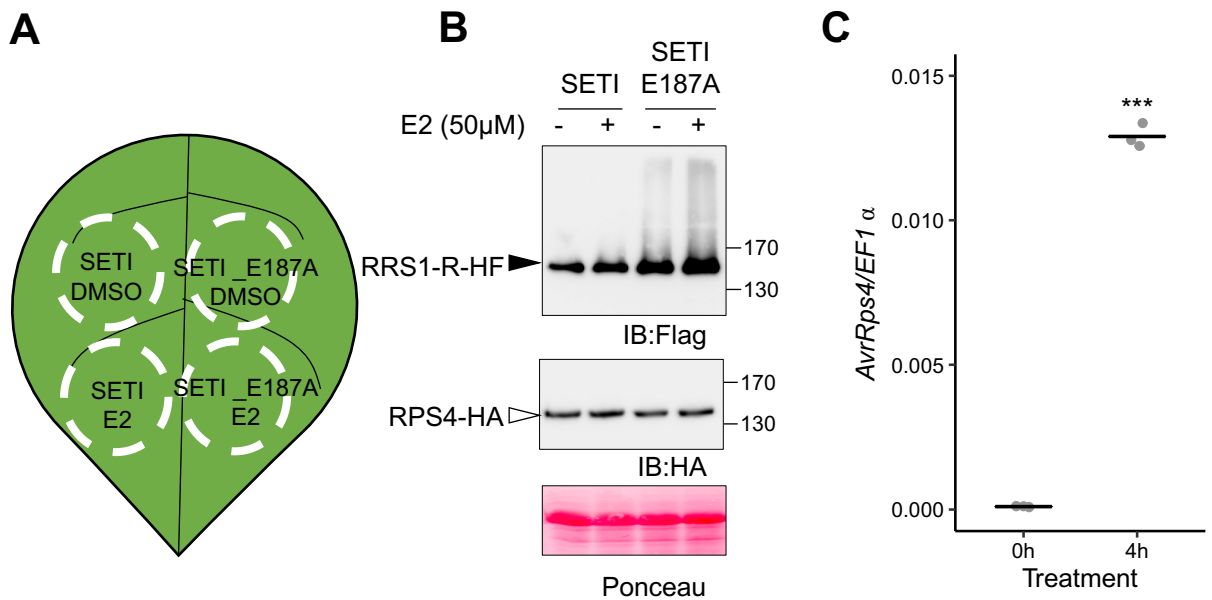
Genotype	Group1	Group2	p	p.adj	p.format	p.signif
Col-0	Col-0 E2	Col-0 Mock	0.621	0.62	0.6213	ns
SET1_WT	SET1_WT E2	SET1_WT Mock	0.000905	0.0018	0.0009	***

1. **diff**: difference between means of the two groups
2. **lower, upper**: the lower and the upper end point of the confidence interval at 95% (default)
3. **p adjusted**: p-value after adjustment for the multiple comparisons.
4. **p**: p-value
5. **p.format**: formatted p value
6. **p.signif**: significance levels



Supplementary Figure S1 GUS-staining activity of synthetic promoters in *N. benthamiana*.

Synthetic promoters At1-At6 were fused to β -glucuronidase (GUS) gene and infiltrated into *N. benthamiana* leaves. GUS expressed under the 35S promoter served as positive control. Mock treatment (infiltration with infiltration buffer) was used as negative control. Leaf samples were collected at 2 days post infiltration (dpi), and GUS staining was performed as in Materials and Methods.

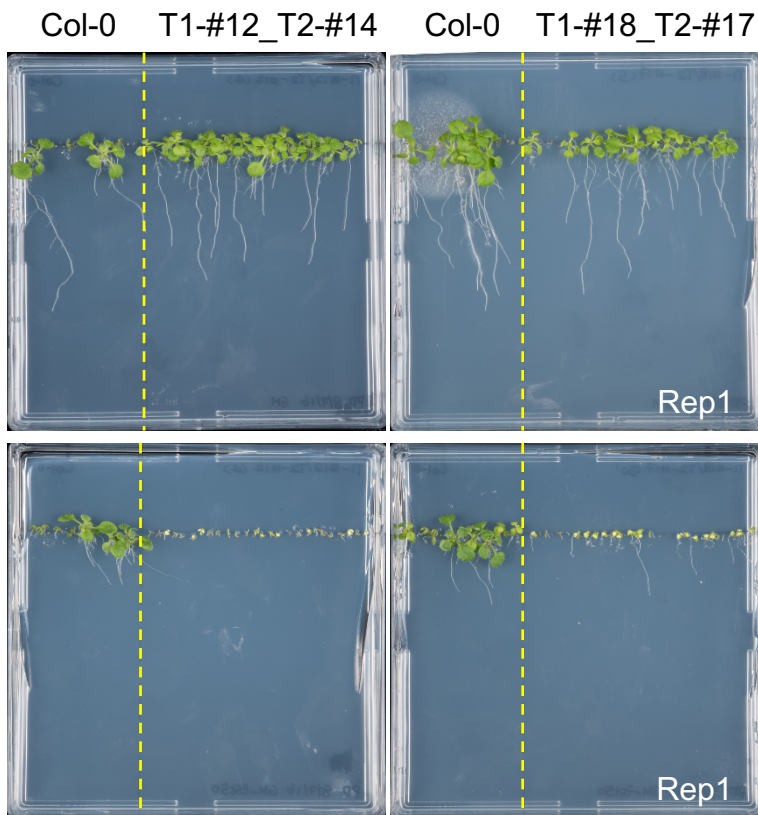
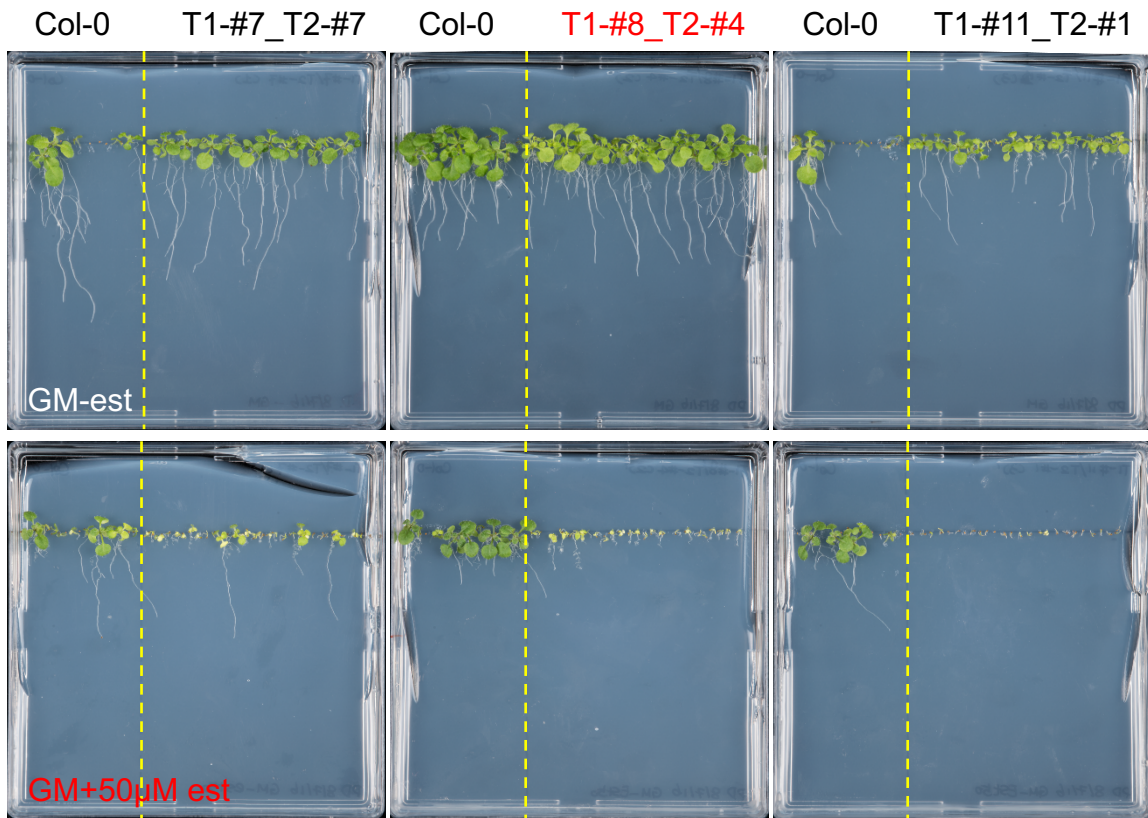


Supplementary Figure S2 Transient expression of Super-ETI (SETI) constructs in *N. benthamiana*.

(A) Schematic diagram of the SETI construct infiltration in *N. benthamiana*. Leaves were infiltrated with *Agrobacterium* containing SETI or SETI_E187A constructs. At 2dpi, leaves were re-infiltrated with 0.1% DMSO or 50 μ M E2 according to the diagram. Samples were taken 6h after infiltration with 0.1% DMSO or 50 μ M E2.

(B) Protein accumulation of RRS1-R-HF and RPS4-HA by transient expression in *N. benthamiana*. Crude extracts of leaf samples from (A) were immunoblotted with Flag antibody (IB:Flag) to detect RRS1-R-HF (black arrowhead) or HA antibody (IB:HA) to detect RPS4-HA (white arrowhead). Ponceau staining of Rubisco large subunits is the loading control.

(C) *AvrRps4* expression after induction with E2 for 4h in the SETI leaves. 5-week old SETI leaves were infiltrated with 50 μ M E2. Samples were collected at 0 and 4hpi for RNA extraction and subsequent qPCR. Expression level is presented as relative to *EF1 α* expression. Each data point represents one technical replicate. Black line represents the mean of the technical replicates. This experiment was repeated three times independently with similar results.



Supplementary Figure S3
SETI T2 lines grown under E2 treatment.

SETI-transformed Arabidopsis transgenic seedlings were sown in GM either containing 50µM E2 or its solvent 0.1% DMSO. Images were taken at 14DAG. Further analysis of SETI lines were performed with the line T1-#8_T2-#4, indicated in red.